Ad genome, inhibit shRNA-mediated RNAi by competition for key components involved in the RNAi pathway (Andersson et al., 2005; Aparicio et al., 2006; Lu and Cullen, 2004; Xu et al., 2007). VA-RNA I and II are about 160 nucleotide-long non-coding RNAs encoded in the Ad genome (bp 10620–10779 and 10876–11038, respectively) (Bhat et al., 1983; Fowlkes and Shenk, 1980; Machitani et al., 2011b; Mathews and Shenk, 1991). After transcription, the VA-RNAs are transported to the cytoplasm by the interaction between their terminal stems and exportin-5, and then processed by an RNase III-type enzyme dicer, resulting in the production of VA-RNA-derived microRNAs (miRNAs) (mivaRNAs) (Andersson et al., 2005; Lu and Cullen, 2004; Xu et al., 2007). After being processed by the dicer, the mivaRNAs are incorporated into an RNA-induced silencing complex (RISC). shRNA is also processed into siRNA through the same pathway. Since VA-RNAs are also expressed from a replication-incompetent first-generation Ad (FG-Ad) vector (Yamaguchi et al., 2010), VA-RNAs transcribed from FG-Ad vectors could inhibit knockdown efficiency of FG-Ad vector-mediated RNAi by competitive inhibition of shRNA processing in several steps, *i.e.*, transport by exportin-5, digestion by the dicer, and incorporation into RISC. Based on these findings, we hypothesized that shRNA-expressing Ad vectors lacking VA-RNA expression exhibit more effective RNAi compared with FG-Ad-shRNA; however, there have been no studies that directly evaluate the inhibitory effects of VA-RNAs transcribed from the Ad vector genome on shRNA-expressing Ad vector (Ad-shRNA)-mediated knockdown.

In the present study, we prepared an shRNA-expressing helper-dependent Ad (HD-Ad) vector, in which almost all viral coding sequences, including VA-RNAs (Palmer and Ng, 2005), were deleted (HD-Ad-shRNA). Titers of HD-Ad-shRNA and FG-AD-shRNA were properly evaluated under the same condition by measuring the expression levels of the green fluorescence protein (GFP) gene, which was inserted into the Ad vector genome. HD-Ad-shRNA showed significantly higher levels of knockdown efficiencies than FG-Ad-shRNA following *in vitro* transduction. Furthermore, shRNA-expressing Ad vectors lacking VA-RNA expression (AdΔVR-shRNA), which are designed to lack only VA-RNA-expression through specific deletion of the transcriptional control elements of VA-RNA, also showed more efficient knockdown than FG-Ad-shRNA.

2. Materials and methods

2.1. Cells

HEK293 (a transformed embryonic kidney cell line), SK HEP-1 (a human hepatoma cell line) and VR293 cells (HEK293 cells inducibly expressing VA-RNA I) were cultured with Dulbecco's modified Eagle's medium supplemented with 10% fetal bovine serum (FBS), streptomycin (100 μg/ml), and penicillin (100 U/ml). WI38 (a normal human lung diploid fibroblast) and 116 cells (Cre recombinase-expressing cells for packaging of HD-Ad vectors) were cultured with Minimum Essential Medium supplemented with 10% FBS, streptomycin (100 μg/ml), and penicillin (100 U/ml).

2.2. Plasmids and virus

HD-Ad vector plasmids, pSTK129-shLuc-GFP, were constructed to express shRNA against firefly luciferase as follows. pHM18-GFP, containing a GFP expression cassette driven by a cytomegalovirus (CMV) promoter, was previously constructed using the pEGFP-N1 plasmid (Clontech, Palo Alto, CA) and a shuttle plasmid, pHM18 (Yamaguchi et al., 2010). pHM18-GFP was digested with *XbaI*/*SphI*, and ligated with the *XbaI*/*SphI* fragment of pHM5-ihU6-Lu (Mizuguchi et al., 2007) after an *SmaI* site of pHM5-ihU6-Lu had been changed into an *XbaI* site by using *XbaI* phosphorylated linkers (New England Biolabs, Beverly, MA), resulting in pHM18-ihU6-Lu-GFP. pHM18-ihU6-Lu-GFP was digested with *NotI*, and the *NotI* fragments were inserted into the *NotI* site of pSTK129 (kindly provided by Dr. Ng Philip) (Palmer and Ng, 2003), resulting in pSTK129-shLuc-GFP. Then, pSTK129-shLuc-GFP was digested with *PmeI*, and the liberated viral genome was transfected into 116 cells expressing Cre recombinase. The HD-Ad vectors were amplified and purified as described previously (Palmer and Ng, 2003). Helper-virus contamination of the HD-Ad vectors was assessed by quantitative real-time PCR, and the level of contamination was estimated to be less than 0.3%. HD-Ad-shp53 was similarly prepared as described above.

The FG-Ad and AdΔVR vectors were constructed by means of an improved *in vitro* ligation method described previously (Mizuguchi and Kay, 1998; Mizuguchi and Kay, 1999; Mizuguchi et al., 2001b; Sakurai et al., 2005) as follows. pHM5 (Mizuguchi and Kay, 1999) was digested with *SphI*/*KpnI*, and ligated with the *SphI*/*KpnI* fragment of pHM18-ihU6-Lu-GFP, resulting in pHM5-ihU6-Lu-GFP. pHM5-ihU6-Lu-GFP was digested with I-*CeuI*/PI-*SceI*, and then ligated with I-*CeuI*/PI-*SceI*-digested pAdHM4 (Mizuguchi and Kay, 1998) or pAdHM4ΔVR (Machitani et al., 2011a), resulting in pAdHM4-shLuc-GFP and pAdHM4ΔVR-shLuc-GFP, respectively. To generate FG-Ad vector particles, pAdHM4-shLuc-GFP was digested with *PacI* to release the recombinant viral genome, and then transfected into HEK293 cells, resulting in FG-Ad-shLuc. AdΔVR-shRNA was prepared as previously described using VR293 cells (Machitani et al., 2011a), instead of HEK293 cells. FG-Ad-shp53 was similarly prepared as described above. The amplified Ad vectors were purified by two rounds of cesium chloride-gradient ultracentrifugation, dialyzed, and stored at −80 °C (Mizuguchi and Kay, 1998). The virus particles (VP) were determined by a spectrophotometrical method (Mizuguchi et al., 2001a). Biological titers, which were based on GFP transduction activity, were determined by serial titration of the vector stocks on SK HEP-1 cells, followed by fluorescence-activated cell sorter (FACS) analysis for GFP-positive cells (Machitani et al., 2011a).

2.3. Preparation of SK HEP-1 transformants expressing luciferase (SK HEP1-Luc)

SK HEP-1 cells were transduced with a lentivirus vector, LV-RVLuP, expressing the Venus fluorescent protein and firefly luciferase as a fusion protein linked with a 2A-self-cleaving peptide (see *Supplementary Information*). The transduced cells expressing the Venus fluorescent protein were sorted by using a FACSAria™ cell sorter (BD Bioscience, San Jose, CA) (Supplemental Fig. 4). The resulting cells were designated SK HEP-1-Luc cells. SK HEP-1-Luc cells were cultured with Dulbecco's modified Eagle's medium supplemented with 10% FBS, streptomycin (100 μg/ml), and penicillin (100 U/ml).

2.4. Determination of small RNA levels incorporated into RISC

RNA incorporated into the RISC was isolated following transduction with Ad vectors using a microRNA Isolation Kit, human argonaute 2 (Ago2) (Wako, Osaka, Japan) according to the manufacturer's instructions. Briefly, Ago2, which is the main component of RISC, was immunoprecipitated by anti-Ago2 antibody to recover RNA in the RISC. After immunoprecipitation, the Ago2-small RNA complex was eluted using elution solution, and small RNA was isolated from the complex using Isogen (Nippon Gene, Tokyo, Japan). Copy numbers of siRNA and VA-RNAs in the isolated RNA (160 ng) were determined by quantitative RT-PCR using Mir-X™ miRNA first-strand synthesis and SYBR® qRT-PCR (Clontech-Takara, Kyoto, Japan) and primers specific for the siLuc, sip53, and

mivaRNAI. The sequences of the primers were as follows: siLuc, 5′-atttcgaagtactcagcgt-3′; sip53, 5′-gtagattaccactggagtc-3′; mivaRNAI, 5′-gacaacgggggagtgctcc-3′.

2.5. Real time RT-PCR analysis

Whole cell lysates for quantitative RT-PCR were prepared from the cells transduced with Ad vectors using a CellAmp® direct RNA Prep Kit (Takara-Bio, Otsu, Japan). After cell lysis, luciferase and p53 mRNA levels were determined by quantitative RT-PCR using a One Step SYBR® PrimeScript® RT-PCR Kit II (Takara-Bio, Otsu, Japan). The primers used for quantitative RT-PCR were as follows: luciferase-F, 5′-tcctatgattatgtccggttatgtaaa-3′; luciferase-R, 5′-tgtagccatccatccttgtcaa-3′; p53-F, 5′-ccgcagtcagatcctagcg-3′; p53-R, 5′-aatcatccattgcttgggacg-3′.

2.6. Luciferase assay

SK HEP-1-Luc cells were transduced with shLuc-expressing Ad vectors. After a 36-h incubation, luciferase activity in the cells was determined using a luciferase assay system (PicaGene LT2.0; Toyo Inki, Tokyo, Japan).

2.7. Western blot analysis

Whole-cell extracts were prepared by suspension of the cells in lysis buffer (20 mM HEPES [pH 7.5], 1% Triton X-100, 2 mM EGTA, 10% glycerol, 5 mM dithiothreitol, 4 mM phenylmethylsulfonyl fluoride) 48 h after transduction. The protein content was measured with a protein assay kit (Bio-Rad, Hercules, CA) using bovine serum albumin as the standard. Protein samples (15 μg) were electrophoresed on 12.5% sodium dodecyl sulfate (SDS)–polyacrylamide gels under reducing conditions, followed by electrotransfer to PVDF membranes (Millipore, Bedford, MA). After blocking with 4% skim milk prepared in TBS-T (tween-20, 0.1%), the membrane was incubated with anti-p53 antibody (Santa Cruz Biotechnology, Santa Cruz, CA), followed by incubation in the presence of horseradish peroxidase (HRP)-labeled anti-mouse IgG antibody (Cell Signaling Technology, Danvers, MA). The membrane was developed with a chemiluminescence kit (ECL Plus Western blotting detection system; Amersham Biosciences, Piscataway, NJ), and then the signals were read with an LAS-3000 imaging system (Fujifilm, Tokyo, Japan).

2.8. Statistical analysis

Statistical significance was determined using Student's *t*-test. Data are presented as the means ± S.D.

3. Results

3.1. Construction of shRNA-expressing FG-Ad and HD-Ad vectors

First, in order to compare the knockdown efficiencies of FG-Ad and HD-Ad vectors expressing shRNA, we constructed the FG-Ad and HD-Ad vectors carrying a U6 promoter-driven shRNA-expression cassette to induce knockdown of target genes (luciferase and human p53 genes). In addition, a CMV promoter-driven GFP-expression cassette was incorporated into the vector genome to precisely determine the titers of these Ad vectors (Fig. 1). We demonstrated that the transduction efficiencies by these Ad vectors at the same multiplicity of infection (MOI) were comparable (Supplemental Figs. 1–3). SK HEP-1 cells were more susceptible to Ad vector-mediated transduction than WI38 cells (Supplemental Figs. 1 and 2).

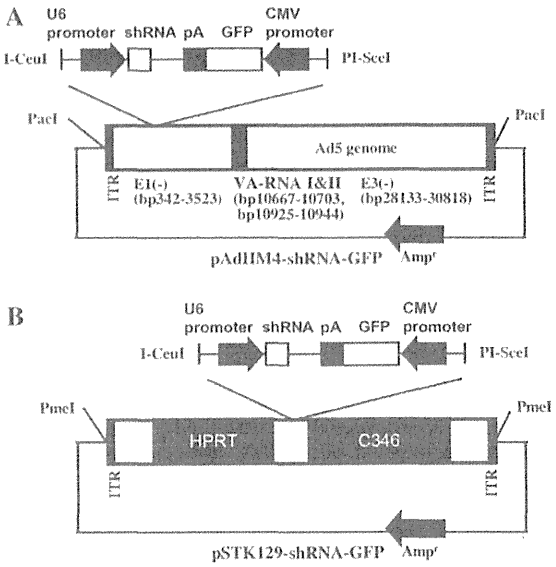

Fig. 1. Vector plasmids for the generation of FG-Ad-shRNA and HD-Ad-shRNA. The structure of the vector plasmids (A) pAdHM4-shRNA-GFP (for FG-Ad-shRNA) and (B) pSTK129-shRNA-GFP (for HD-Ad-shRNA). pA: bovine growth hormone (BGH) poly A sequence; ITR: inverted terminal repeat; Amp^r: ampicillin resistance gene; HPRT: intron region of human genomic HPRT stuffer sequence; C346: cosmid C346 human genomic stuffer sequence.

3.2. Copy numbers of siRNA and VA-RNA in the RISC

Next, in order to examine whether incorporation of siRNA which was processed from the shRNA into RISC was inhibited by VA-RNAs, SK HEP-1 cells constitutively expressing firefly luciferase (SK HEP-1-Luc cells) were transduced with a FG-Ad vector expressing shRNA against the luciferase gene (shLuc) (FG-Ad-shLuc), and then, the copy numbers of siLuc (the processed form of shLuc) and mivaRNAI in the RISC were determined by real-time RT-PCR. The analysis demonstrated that the copy numbers of siLuc and mivaRNAI in the RISC were almost comparable following the transduction with FG-Ad-shLuc at all the MOIs (Fig. 2A). On the other hand, when the cells were transduced with an HD-Ad vector expressing shLuc (HD-Ad-shLuc), a significantly higher amount of siLuc was found in the RISC, compared with FG-Ad-shLuc (Fig. 2B). Transduction with HD-Ad-shLuc resulted in an approximately 5-fold higher amount of siLuc in the RISC than that with FG-Ad-shLuc at the MOIs of 1, 3, and 10 (Fig. 2B). A significantly higher amount of sip53, which is processed from an shRNA against human p53 (shp53), was also found in the RISC for an HD-Ad vector expressing shp53 (HD-Ad-shp53), compared with an FG-Ad vector expressing shp53 (FG-Ad-shp53), in WI38 cells (Fig. 2C). These results suggest that the competition between shRNA and VA-RNAs, both of which are transcribed from the same Ad vector genome, in the processing steps leads to the lower copy numbers of siRNA in the RISC when transduced with FG-Ad-shRNA, compared with HD-Ad-shRNA.

3.3. Efficient knockdown of target genes by HD-Ad-shRNA

Next, to evaluate the effect of VA-RNAs on the knockdown efficiencies of shRNA-expressing Ad vectors, SK HEP-1-Luc cells were transduced with FG-Ad-shLuc or HD-Ad-shLuc at an MOI of 1, 3, or 10. In this experiment, we confirmed that a FG-Ad vector expressing shRNA against the other gene (p53 gene) (FG-Ad-shp53) did not knockdown luciferase expression (Supplemental Fig. 4). HD-Ad-shLuc mediated an approximately 10% increase in the efficiency of knockdown of luciferase mRNA at the MOIs of 3 and 10 (Fig. 3A)

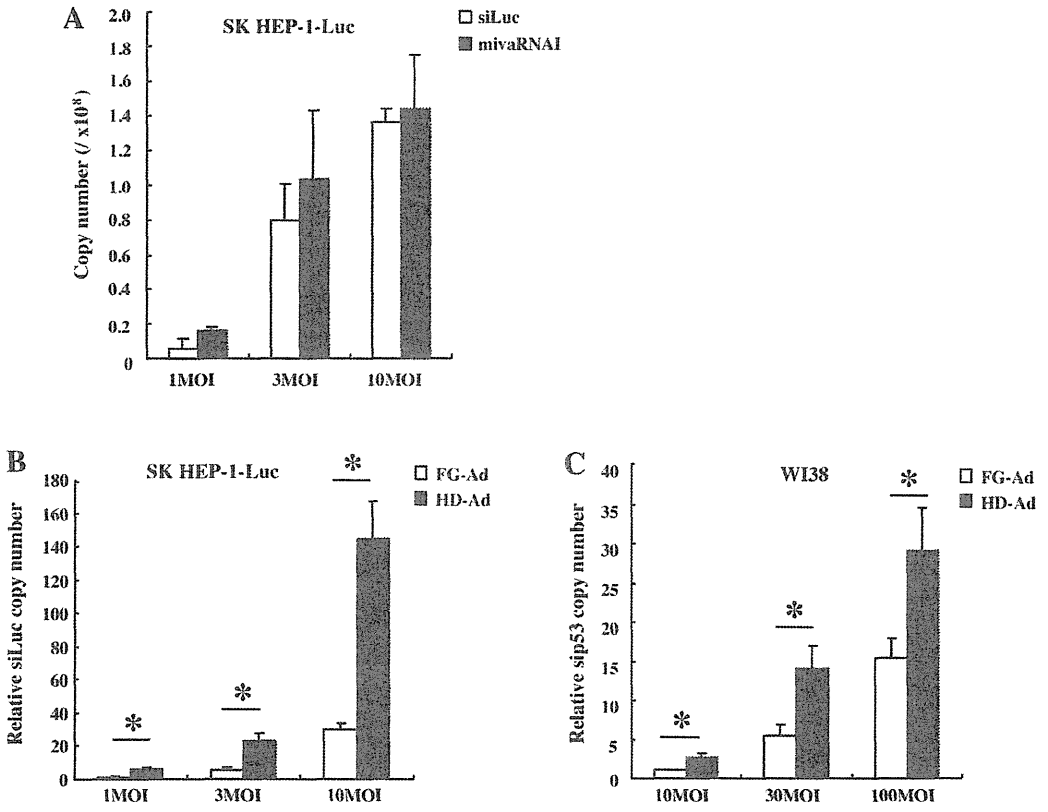

Fig. 2. Comparison of small RNA levels incorporated into RISC.
(A) Copy numbers of siLuc (the processed form of shLuc) and mivaRNAI in the RNA-induced silencing complex (RISC) recovered from SK HEP-1-Luc cells following transduction with FG-Ad-shLuc-GFP. (B) Copy numbers of siLuc and mivaRNAI in the RISC recovered from SK HEP-1-Luc cells following transduction with HD-Ad-shLuc-GFP. SK HEP-1-Luc cells were transduced with FG-Ad-shLuc or HD-Ad-shLuc at a multiplicity of infection (MOI) of 1, 3 or 10. Total RNA was recovered from the RNA-induced silencing complex (RISC) 36 h after transduction with Ad vectors. Copy numbers of siLuc and mivaRNAI were determined by quantitative RT-PCR. The copy number of siLuc in the RISC following transduction with FG-Ad-shLuc at an MOI of 1 was normalized to 1. (C) Copy numbers of sip53 in the RISC recovered from WI38 cells following transduction with FG-Ad-shp53 or HD-Ad-shp53. WI38 cells were transduced with FG-Ad-shp53 or HD-Ad-shp53 at an MOI of 10, 30 or 100. Total RNA was isolated from the RISC 48 h after transduction, and copy numbers of sip53 were determined by quantitative RT-PCR. The copy number of sip53 in the RISC following transduction with FG-Ad-shp53 at an MOI of 10 was normalized to 1. These experiments were repeated at least three times, and representative data are shown. All the data are expressed as means ± S.D. ($n = 3$). *$p < 0.01$.

and in the efficiency of knockdown of luciferase activity levels at all MOIs (Fig. 3B), compared with FG-Ad-shLuc. Significantly higher knockdown efficiencies were also found for HD-Ad-shp53 than FG-Ad-shp53 in WI38 cells (Fig. 4A and B). Surprisingly, the p53-knockdown efficiencies were more greatly improved by the use of an HD-Ad vector, compared with the luciferase-knockdown efficiencies, although the increases in the copy numbers of siLuc in the RISC were larger than those of sip53 by the use of an HD-Ad vector. A 37% increase in the p53-knockdown efficiency was observed when the WI38 cells were transduced with HD-Ad-shp53 at an MOI of 100, compared with FG-Ad-shp53 (Fig. 4A). Significantly more efficient knockdown of p53 was also found for HD-Ad-shp53 than FG-Ad-shp53 in SK HEP-1 (Supplemental Fig. 5). These results indicate that HD-Ad-shRNA shows higher levels of knockdown efficiencies than FG-Ad-shRNA.

3.4. Efficient knockdown of target genes by AdΔVR-shRNA

As described above, HD-Ad-shRNA showed higher levels of knockdown efficiencies than FG-Ad-shRNA; however, it is unclear whether the deletion of VA-RNAs really contributed to the enhanced knockdown efficiencies of HD-Ad-shRNA, because HD-Ad vectors are devoid of all viral genes, including VA-RNAs (Palmer and Ng, 2005). Therefore, in order to further demonstrate that VA-RNAs inhibit shRNA-mediated knockdown, the knockdown efficiencies of shRNA-expressing AdΔVR vectors were examined (Fig. 5A). AdΔVR vectors, which were previously developed by our group, lack VA-RNA expression due to deletion of the transcriptional control elements for VA-RNA expression (Machitani et al., 2011a). We confirmed that the transduction efficiencies of FG-Ad- and AdΔVR-shLuc at the same MOIs were comparable (Supplemental Fig. 3). Real-time RT-PCR analysis demonstrated that an approximately 2-fold higher amount of siLuc was found in the RISC following transduction with AdΔVR-shLuc, compared with FG-Ad-shLuc at an MOI of 10 (Fig. 5B). Furthermore, AdΔVR-shLuc showed 9.7% higher knockdown efficiencies than FG-Ad-shLuc at an MOI of 10 (Fig. 5C and D), suggesting that the deletion of VA-RNAs led to an enhancement in the knockdown efficiency of shRNA-expressing Ad vectors.

4. Discussion

The aim of this study is to examine whether an shRNA-expressing Ad vector-mediated knockdown was inhibited by VA-RNAs transcribed from the same Ad vector genome. So far, previous studies have reported the suppression of shRNA-mediated RNAi by VA-RNAs (Andersson et al., 2005; Lu and Cullen, 2004); however, shRNA and VA-RNAs were expressed separately from the two different plasmids in these studies. In this study, we constructed shRNA-expressing HD-Ad vectors and AdΔVR vectors,

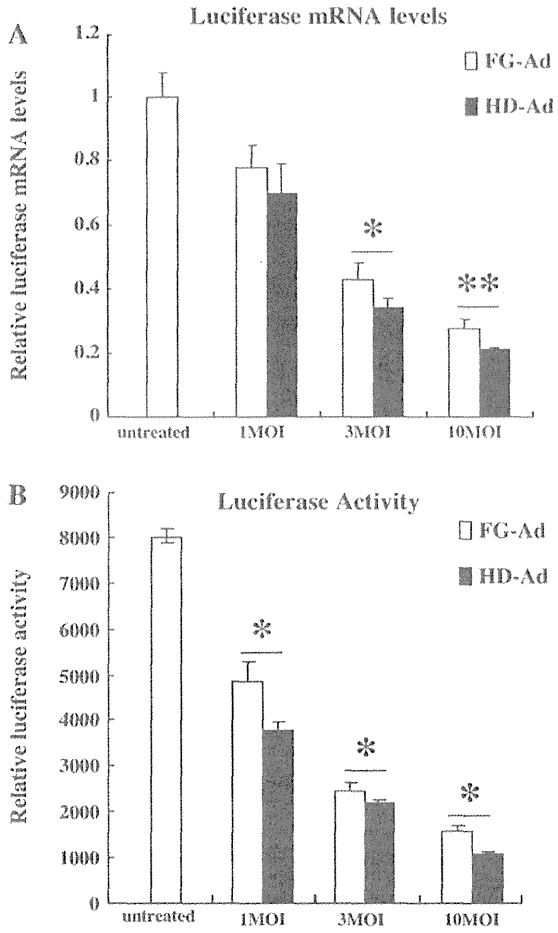

Fig. 3. Knockdown efficiencies of FG-Ad-shLuc and HD-Ad-shLuc in SK HEP-1-Luc cells.
Luciferase mRNA levels (A) and luciferase activity (B) following transduction with FG-Ad-shLuc or HD-Ad-shLuc in SK HEP-1-Luc cells. SK HEP-1-Luc cells were transduced with FG-Ad-shLuc or HD-Ad-shLuc at a multiplicity of infection (MOI) of 1, 3 or 10. After a 36-h incubation, mRNA levels of the luciferase gene and luciferase activity were determined. $^{*}p < 0.05$, $^{**}p < 0.01$.

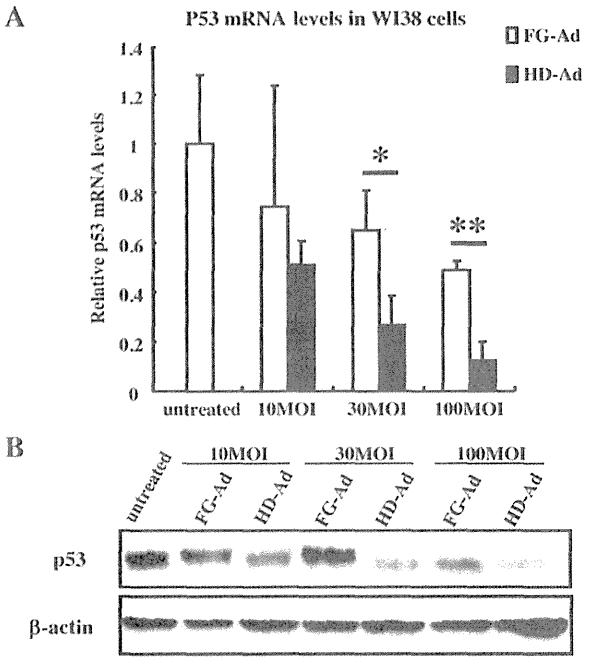

Fig. 4. Knockdown efficiencies of FG-Ad-shp53 and HD-Ad-shp53 in WI38 cells.
(A) p53 mRNA levels following transduction with FG-Ad-shLuc or HD-Ad-shLuc in WI38 cells. Cells were transduced with FG-Ad-shp53 or HD-Ad-shp53 at an MOI of 10, 30 or 100. After a 48-h incubation, mRNA levels of the p53 gene were determined by quantitative RT-PCR. All the data are expressed as the means ± S.D. ($n = 4$). (B) p53 protein levels following transduction with FG-Ad-shLuc or HD-Ad-shLuc in WI38 cells. WI38 cells were transduced with FG-Ad-shp53 or HD-Ad-shp53 at an MOI of 10, 30 or 100. After a 48-h incubation, Western blot analysis for p53 was performed. These experiments were repeated at least three times, and representative data are shown. $^{*}p < 0.05$, $^{**}p < 0.01$.

which do not express VA-RNAs, and evaluated the knockdown efficiencies. shRNA-expressing HD-Ad vectors and AdΔVR vectors exhibited higher knockdown efficiencies than shRNA-expressing FG-Ad vectors in this study. VA-RNAs and miRNA/shRNA shares the common processing steps, including export into cytosol, digestion by dicer, and loading into RISC. Lu et al. demonstrated that VA-RNAs competitively inhibit miRNA biogenesis (Lu and Cullen, 2004). In addition, VA-RNAs have recently been demonstrated to suppress dicer expression by competitive binding for exportin-5 between dicer mRNA (Bennasser et al., 2011). Therefore, HD-Ad- and AdΔVR-shRNA do not inhibit miRNA processing due to the lack of VA-RNA expression. This property is highly crucial, especially for shRNA-expressing Ad vectors. Grimm et al. reported that overexpression of shRNA in the liver resulted in suppression of miRNA processing, leading to severe hepatotoxicity (Grimm et al., 2006). Expression of both VA-RNAs and shRNA might inhibit miRNA processing more severely than shRNA alone.

The present study suggests that HD-Ad-shRNA and AdΔVR-shRNA have greater potential to efficiently induce RNAi effects, compared with FG-Ad-shRNA. The application of HD-Ad- and AdΔVR-shRNA will be helpful for decreasing the viral dose required to achieve an RNAi-mediated therapeutic effect. Furthermore, HD-Ad-shRNA eliminates the possibility of leaky expression of the viral gene and subsequent toxic effects, because HD-Ad vectors delete almost all of the viral coding sequence. These characteristics could contribute to a reduction of the immunological side effects caused by the Ad vector itself (Chen et al., 2003; Jooss and Chirmule, 2003; Koizumi et al., 2007; Liu and Muruve, 2003; Muruve, 2004; Sakurai et al., 2008; Xu et al., 2005; Yamaguchi et al., 2007).

As described above, HD-Ad and AdΔVR vectors are superior to FG-Ad vectors in the shRNA-mediated knockdown efficiencies; however, the expression of VA-RNAs from the plasmids resulted in higher levels of reduction in the shRNA-mediated knockdown efficiencies, compared with the differences in the knockdown efficiencies between FG-Ad vectors and HD-Ad vectors or AdΔVR vectors shown in the present study. Andersson et al. reported that knockdown efficiencies by plasmids expressing shLuc were attenuated from about 80% to 30% by co-transfection with plasmids expressing VA-RNAs (Andersson et al., 2005). Similar results were shown by Lu et al. (Lu and Cullen, 2004) This is probably because the expression levels of VA-RNAs per plasmid-transfected cell were higher than those per Ad vector-transduced cell, although the numbers of VA-RNA-expressing cells were lower for the plasmid transfection than for transduction with an Ad vector.

There was no apparent correlation between the knockdown efficiencies of shRNA-expressing Ad vectors and the copy numbers of the siRNA in the RISC. About 5-fold higher amounts of siLuc were found in the RISC following transduction with HD-Ad-shLuc, compared with FG-Ad-shLuc; however, HD-Ad-shLuc showed only a 7.4% increase in the knockdown efficiencies compared with FG-Ad-shLuc (Fig. 3A and B). Although AdΔVR-shLuc mediated about 2-fold elevation in the copy number of siLuc in the RISC at MOI of

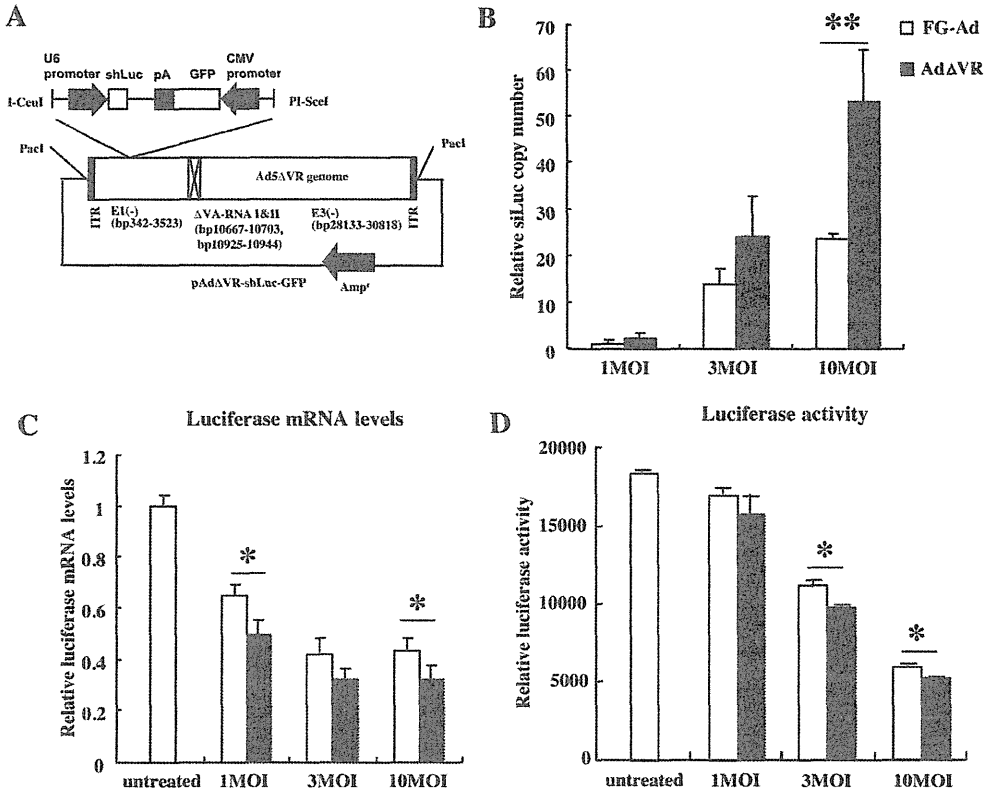

Fig. 5. Knockdown efficiencies of FG-Ad-shLuc and AdΔVR-shLuc.
(A) The structure of the vector plasmid, pAdΔVR-shLuc-GFP. pA: bovine growth hormone (BGH) pA sequence; ITR: inverted terminal repeat; Amp^r: ampicillin resistance gene. (B) Copy numbers of siLuc in the RISC recovered from SK HEP-1-Luc cells following transduction with FG-Ad-shLuc or AdΔVR-shLuc. SK HEP-1-Luc cells were transduced with FG-Ad-shLuc or AdΔVR-shLuc at a multiplicity of infection (MOI) of 1, 3 or 10. After a 36-h incubation, total RNA was extracted from the RISC. The copy numbers of siLuc were determined by quantitative RT-PCR. The copy number of siLuc in the RNA-induced silencing complex (RISC) following transduction with FG-Ad-shLuc at an MOI of 1 was normalized to 1. The data are expressed as the means ± S.D. ($n = 3$). (C, D) Luciferase mRNA levels (C) and luciferase activity (D) following transduction with FG-Ad-shLuc or AdΔVR-shLuc. SK HEP-1-Luc cells were transduced with FG-Ad-shLuc or HD-Ad-shLuc at an MOI of 1, 3 or 10. After a 36-h incubation, mRNA levels of the luciferase gene and luciferase production were determined. These experiments were repeated at least three times, and representative data are shown. The data are expressed as the means ± S.D. ($n = 4$). $^*p < 0.05$, $^{**}p < 0.01$.

10, compared with FG-Ad-shLuc, approximately 10% increase in the knockdown efficiency was found for AdΔVR-shLuc. On the other hand, HD-Ad-shp53 showed a 37.3% increase in the knockdown efficiencies in WI38 cells, compared with FG-Ad-shp53 (Fig. 4A), although there was an approximately 2-fold increase in the copy number of sip53 following transduction with HD-Ad-shp53, compared with FG-Ad-shp53 (Fig. 2C). It might be difficult to largely improve the knockdown efficiency of shLuc used in this study by deletion of VA-RNA gene from the Ad vector genome because sufficiently efficient knockdown of luciferase gene was obtained even by FG-Ad-shLuc. By contrast, knockdown of p53 by FG-Ad-shp53 was less efficient than that of luciferase by FG-Ad-shLuc. Therefore, deletion of VA-RNA gene more largely elevated the knockdown efficiencies of shp53. A previous study demonstrated that overexpression of Ago2 more dramatically improved the knockdown efficiency of less efficient siRNA than high potent siRNA (Diederichs et al., 2008). The degree of increase in the knockdown efficiencies of HD-Ad-shRNA would be different depending on target genes, transduced cells, and/or knockdown capacity of shRNA.

5. Conclusions

In summary, we have demonstrated that VA-RNAs expressed from the Ad vector genome inhibited efficient knockdown by Ad vector-mediated RNAi. To the best of our knowledge, this is the first study demonstrating the effects of Ad vector-derived VA-RNAs on Ad vector-mediated RNAi. HD-Ad and AdΔVR vectors are highly promising as a platform for shRNA-mediated knockdown and to provide important clues for the improvement of RNAi-mediated knockdown systems using Ad vectors.

Acknowledgements

We thank Dr. Miyoshi for providing the lentivirus vector construct (CS-CDF-RVLuP). This work was supported in part by a grant-in-aid for Research on Publicly Essential Drugs and Medical Devices (KHB1009) to F.S. and to H.M. from the Japan Health Sciences Foundation, and by a grant-in aid for Young Scientists (A) from the Ministry of Education, Culture, Sports, Sciences, and Technology (MEXT) of Japan. M. Machitani is a Research Fellow of the Japan Society for Promotion of Science.

Appendix A. Supplementary data

Supplementary data associated with this article can be found, in the online version, at http://dx.doi.org/10.1016/j.virusres.2013.09.021.

References

Andersson, M.G., Haasnoot, P.C., Xu, N., Berenjian, S., Berkhout, B., Akusjarvi, G., 2005. Suppression of RNA interference by adenovirus virus-associated RNA. J. Virol. 79 (15), 9556–9565.

Aparicio, O., Razquin, N., Zaratiegui, M., Narvaiza, I., Fortes, P., 2006. Adenovirus virus-associated RNA is processed to functional interfering RNAs involved in virus production. J. Virol. 80 (3), 1376–1384.
Benihoud, K., Yeh, P., Perricaudet, M., 1999. Adenovirus vectors for gene delivery. Curr. Opin. Biotechnol. 10 (5), 440–447.
Bennasser, Y., Chable-Bessia, C., Triboulet, R., Gibbings, D., Gwizdek, C., Dargemont, C., Kremer, E.J., Voinnet, O., Benkirane, M., 2011. Competition for XPO5 binding between Dicer mRNA, pre-miRNA and viral RNA regulates human Dicer levels. Nat. Struct. Mol. Biol. 18 (3), 323–327.
Bhat, R.A., Metz, B., Thimmappaya, B., 1983. Organization of the noncontiguous promoter components of adenovirus VAI RNA gene is strikingly similar to that of eucaryotic tRNA genes. Mol. Cell. Biol. 3 (11), 1996–2005.
Chen, D., Murphy, B., Sung, R., Bromberg, J.S., 2003. Adaptive and innate immune responses to gene transfer vectors: role of cytokines and chemokines in vector function. Gene Ther. 10 (11), 991–998.
Diederichs, S., Jung, S., Rothenberg, S.M., Smolen, G.A., Mlody, B.G., Haber, D.A., 2008. Coexpression of Argonaute-2 enhances RNA interference toward perfect match binding sites. Proc. Natl. Acad. Sci. USA. 105 (27), 9284–9289.
Fowlkes, D.M., Shenk, T., 1980. Transcriptional control regions of the adenovirus VAI RNA gene. Cell 22 (2 Pt 2), 405–413.
Giering, J.C., Grimm, D., Storm, T.A., Kay, M.A., 2008. Expression of shRNA from a tissue-specific pol II promoter is an effective and safe RNAi therapeutic. Mol. Ther. 16 (9), 1630–1636.
Grimm, D., Kay, M.A., 2007. RNAi and gene therapy: a mutual attraction. Hematol. Am. Soc. Hematol. Educ. Program, 473–481.
Grimm, D., Streetz, K.L., Jopling, C.L., Storm, T.A., Pandey, K., Davis, C.R., Marion, P., Salazar, F., Kay, M.A., 2006. Fatality in mice due to oversaturation of cellular microRNA/short hairpin RNA pathways. Nature 441 (7092), 537–541.
Hosono, T., Mizuguchi, H., Katayama, K., Koizumi, N., Kawabata, K., Yamaguchi, T., Nakagawa, S., Watanabe, Y., Mayumi, T., Hayakawa, T., 2005. RNA interference of PPARgamma using fiber-modified adenovirus vector efficiently suppresses preadipocyte-to-adipocyte differentiation in 3T3-L1 cells. Gene 348, 157–165.
Hosono, T., Mizuguchi, H., Katayama, K., Xu, Z.L., Sakurai, F., Ishii-Watabe, A., Kawabata, K., Yamaguchi, T., Nakagawa, S., Mayumi, T., Hayakawa, T., 2004. Adenovirus vector-mediated doxycycline-inducible RNA interference. Hum. Gene Ther. 15 (8), 813–819.
Jooss, K., Chirmule, N., 2003. Immunity to adenovirus and adeno-associated viral vectors: implications for gene therapy. Gene Ther. 10 (11), 955–963.
Koizumi, N., Yamaguchi, T., Kawabata, K., Sakurai, F., Sasaki, T., Watanabe, Y., Hayakawa, T., Mizuguchi, H., 2007. Fiber-modified adenovirus vectors decrease liver toxicity through reduced IL-6 production. J. Immunol. 178 (3), 1767–1773.
Liu, Q., Muruve, D.A., 2003. Molecular basis of the inflammatory response to adenovirus vectors. Gene Ther. 10 (11), 935–940.
Lu, S., Cullen, B.R., 2004. Adenovirus VA1 noncoding RNA can inhibit small interfering RNA and MicroRNA biogenesis. J. Virol. 78 (23), 12868–12876.
Machitani, M., Katayama, K., Sakurai, F., Matsui, H., Yamaguchi, T., Suzuki, T., Miyoshi, H., Kawabata, K., Mizuguchi, H., 2011a. Development of an adenovirus vector lacking the expression of virus-associated RNAs. J. Control Release 154 (3), 285–289.
Machitani, M., Yamaguchi, T., Shimizu, K., Sakurai, F., Katayama, K., Kawabata, K., Mizuguchi, H., 2011b. Adenovirus vector-derived VA-RNA-mediated innate immune responses. Pharmaceutics 3, 338–353.
Mathews, M.B., Shenk, T., 1991. Adenovirus virus-associated RNA and translation control. J. Virol. 65 (11), 5657–5662.
Mizuguchi, H., Funakoshi, N., Hosono, T., Sakurai, F., Kawabata, K., Yamaguchi, T., Hayakawa, T., 2007. Rapid construction of small interfering RNA-expressing adenoviral vectors on the basis of direct cloning of short hairpin RNA-coding DNAs. Hum. Gene Ther. 18 (1), 74–80.
Mizuguchi, H., Kay, M.A., 1998. Efficient construction of a recombinant adenovirus vector by an improved in vitro ligation method. Hum. Gene Ther. 9 (17), 2577–2583.
Mizuguchi, H., Kay, M.A., 1999. A simple method for constructing E1- and E1/E4-deleted recombinant adenoviral vectors. Hum. Gene Ther. 10 (12), 2013–2017.
Mizuguchi, H., Kay, M.A., Hayakawa, T., 2001a. In vitro ligation-based cloning of foreign DNAs into the E3 and E1 deletion regions for generation of recombinant adenovirus vectors. Biotechniques 30 (5), 1112–1114, 1116.
Mizuguchi, H., Koizumi, N., Hosono, T., Utoguchi, N., Watanabe, Y., Kay, M.A., Hayakawa, T., 2001b. A simplified system for constructing recombinant adenoviral vectors containing heterologous peptides in the HI loop of their fiber knob. Gene Ther. 8 (9), 730–735.
Motegi, Y., Katayama, K., Sakurai, F., Kato, T., Yamaguchi, T., Matsui, H., Takahashi, M., Kawabata, K., Mizuguchi, H., 2011. An effective gene-knockdown using multiple shRNA-expressing adenovirus vectors. J. Control Release 153 (2), 149–153.
Muruve, D.A., 2004. The innate immune response to adenovirus vectors. Hum. Gene Ther. 15 (12), 1157–1166.
Palmer, D., Ng, P., 2003. Improved system for helper-dependent adenoviral vector production. Mol. Ther. 8 (5), 846–852.
Palmer, D.J., Ng, P., 2005. Helper-dependent adenoviral vectors for gene therapy. Hum. Gene Ther. 16 (1), 1–16.
Sakurai, F., Kawabata, K., Yamaguchi, T., Hayakawa, T., Mizuguchi, H., 2005. Optimization of adenovirus serotype 35 vectors for efficient transduction in human hematopoietic progenitors: comparison of promoter activities. Gene Ther. 12 (19), 1424–1433.
Sakurai, H., Kawabata, K., Sakurai, F., Nakagawa, S., Mizuguchi, H., 2008. Innate immune response induced by gene delivery vectors. Int. J. Pharm. 354 (1-2), 9–15.
Scherer, L.J., Rossi, J.J., 2003. Approaches for the sequence-specific knockdown of mRNA. Nat. Biotechnol. 21 (12), 1457–1465.
Tuschl, T., 2002. Expanding small RNA interference. Nat. Biotechnol. 20 (5), 446–448.
Xu, N., Segerman, B., Zhou, X., Akusjarvi, G., 2007. Adenovirus virus-associated RNAII-derived small RNAs are efficiently incorporated into the rna-induced silencing complex and associate with polyribosomes. J. Virol. 81 (19), 10540–10549.
Xu, Z.L., Mizuguchi, H., Sakurai, F., Koizumi, N., Hosono, T., Kawabata, K., Watanabe, Y., Yamaguchi, T., Hayakawa, T., 2005. Approaches to improving the kinetics of adenovirus-delivered genes and gene products. Adv. Drug. Deliver. Rev. 57 (5), 781–802.
Yamaguchi, T., Kawabata, K., Koizumi, N., Sakurai, F., Nakashima, K., Sakurai, H., Sasaki, T., Okada, N., Yamanishi, K., Mizuguchi, H., 2007. Role of MyD88 and TLR9 in the innate immune response elicited by serotype 5 adenoviral vectors. Hum. Gene Ther. 18 (8), 753–762.
Yamaguchi, T., Kawabata, K., Kouyama, E., Ishii, K.J., Katayama, K., Suzuki, T., Kurachi, S., Sakurai, F., Akira, S., Mizuguchi, H., 2010. Induction of type I interferon by adenovirus-encoded small RNAs. Proc. Natl. Acad. Sci. USA. 107 (40), 17286–17291.

© 2014. Published by The Company of Biologists Ltd | Development (2014) 141, 91-100 doi:10.1242/dev.103168

RESEARCH ARTICLE

STEM CELLS AND REGENERATION

CCAAT/enhancer binding protein-mediated regulation of TGFβ receptor 2 expression determines the hepatoblast fate decision

Kazuo Takayama[1,2,3], Kenji Kawabata[4], Yasuhito Nagamoto[1,2], Mitsuru Inamura[1], Kazuo Ohashi[5], Hiroko Okuno[1], Tomoko Yamaguchi[4], Katsuhisa Tashiro[4], Fuminori Sakurai[1], Takao Hayakawa[6], Teruo Okano[5], Miho Kusada Furue[7,8] and Hiroyuki Mizuguchi[1,2,3,9,*]

ABSTRACT

Human embryonic stem cells (hESCs) and their derivatives are expected to be used in drug discovery, regenerative medicine and the study of human embryogenesis. Because hepatocyte differentiation from hESCs has the potential to recapitulate human liver development *in vivo*, we employed this differentiation method to investigate the molecular mechanisms underlying human hepatocyte differentiation. A previous study has shown that a gradient of transforming growth factor beta (TGFβ) signaling is required to segregate hepatocyte and cholangiocyte lineages from hepatoblasts. Although CCAAT/enhancer binding proteins (c/EBPs) are known to be important transcription factors in liver development, the relationship between TGFβ signaling and c/EBP-mediated transcriptional regulation in the hepatoblast fate decision is not well known. To clarify this relationship, we examined whether c/EBPs could determine the hepatoblast fate decision via regulation of TGFβ receptor 2 (TGFBR2) expression in the hepatoblast-like cells differentiated from hESCs. We found that *TGFBR2* promoter activity was negatively regulated by c/EBPα and positively regulated by c/EBPβ. Moreover, c/EBPα overexpression could promote hepatocyte differentiation by suppressing TGFBR2 expression, whereas c/EBPβ overexpression could promote cholangiocyte differentiation by enhancing TGFBR2 expression. Our findings demonstrated that c/EBPα and c/EBPβ determine the lineage commitment of hepatoblasts by negatively and positively regulating the expression of a common target gene, *TGFBR2*, respectively.

KEY WORDS: Hepatoblasts, c/EBP, CEBP, Human ESCs

INTRODUCTION

Many animal models, such as chick, *Xenopus*, zebrafish and mouse, have been used to investigate the molecular mechanisms of liver development. Because many functions of the key molecules in liver development are conserved in these species, studies on liver development in these animals can be highly informative with respect that in humans. However, some functions of important molecules in liver development might differ between human and other species. Although analysis using genetically modified mice has been successfully performed, it is not of course possible to perform genetic experiments to elucidate molecular mechanisms of liver development in human. Pluripotent stem cells, such as human embryonic stem cells (hESCs), are expected to overcome some of these problems in the study of human embryogenesis, including liver development, because the gene expression profiles of this model are similar to those in normal liver development (Agarwal et al., 2008; DeLaForest et al., 2011).

During liver development, hepatoblasts differentiate into hepatocytes and cholangiocytes. A previous study has shown that a high concentration of transforming growth factor beta (TGFβ) could give rise to cholangiocyte differentiation from hepatoblasts (Clotman et al., 2005). To transmit the TGFβ signaling, TGFβ receptor 2 (TGFBR2) has to be stimulated by TGFβ1, TGFβ2 or TGFβ3 (Kitisin et al., 2007). TGFβ binding to the extracellular domain of TGFBR2 induces a conformational change, resulting in the phosphorylation and activation of TGFBR1. TGFBR1 phosphorylates SMAD2 or SMAD3, which binds to SMAD4, and then the SMAD complexes move into the nucleus and function as transcription factors to express various kinds of differentiation-related genes (Kitisin et al., 2007). Although the function of TGFBR2 in regeneration of the adult liver has been thoroughly examined (Oe et al., 2004), the function of TGFBR2 in the hepatoblast fate decision has not been elucidated.

CCAAT/enhancer binding protein (c/EBP) transcription factors play decisive roles in the differentiation of various cell types, including hepatocytes (Tomizawa et al., 1998; Yamasaki et al., 2006). The analysis of *c/EBPα* (*Cebpa*) knockout mice has shown that many abnormal pseudoglandular structures, which co-express antigens specific for both hepatocytes and cholangiocytes, are present in the liver parenchyma (Tomizawa et al., 1998). These data demonstrated that c/EBPα plays an important role in hepatocyte differentiation. It is also known that the suppression of c/EBPα expression in periportal hepatoblasts stimulates cholangiocyte differentiation (Yamasaki et al., 2006). Although the function of c/EBPα in liver development is well known, the relationship between TGFβ signaling and c/EBPα-mediated transcriptional regulation in the hepatoblast fate decision is poorly understood. c/EBPβ is also known to be an important factor for liver function (Chen et al., 2000), although the function of c/EBPβ in the cell fate decision of hepatoblasts is not well known. c/EBPα and c/EBPβ bind to the same DNA binding site. However, the promoter activity of hepatocyte-specific genes, such as those encoding hepatocyte nuclear factor 6 (HNF6, also known as ONECUT1) and UGT2B1,

[1]Laboratory of Biochemistry and Molecular Biology, Graduate School of Pharmaceutical Sciences, Osaka University, Osaka 565-0871, Japan. [2]Laboratory of Hepatocyte Differentiation, National Institute of Biomedical Innovation, Osaka 567-0085, Japan. [3]iPS Cell-based Research Project on Hepatic Toxicity and Metabolism, Graduate School of Pharmaceutical Sciences, Osaka University, Osaka 565-0871, Japan. [4]Laboratory of Stem Cell Regulation, National Institute of Biomedical Innovation, Osaka 567-0085, Japan. [5]Institute of Advanced Biomedical Engineering and Science, Tokyo Women's Medical University, Tokyo 162-8666, Japan. [6]Pharmaceutical Research and Technology Institute, Kinki University, Osaka 577-8502, Japan. [7]Laboratory of Embryonic Stem Cell Cultures, Department of Disease Bioresources Research, National Institute of Biomedical Innovation, Osaka 567-0085, Japan. [8]Department of Embryonic Stem Cell Research, Field of Stem Cell Research, Institute for Frontier Medical Sciences, Kyoto University, Kyoto 606-8507, Japan. [9]The Center for Advanced Medical Engineering and Informatics, Osaka University, Osaka 565-0871, Japan.

*Author for correspondence (mizuguch@phs.osaka-u.ac.jp)

Received 27 August 2013; Accepted 3 October 2013

is positively regulated by c/EBPα but not c/EBPβ (Hansen et al., 1998; Plumb-Rudewiez et al., 2004), suggesting that the functions of c/EBPα and c/EBPβ in the hepatoblast fate decision might be different.

In the present study, we first examined the function of TGFBR2 in the hepatoblast fate decision using hESC-derived hepatoblast-like cells, which have the ability to self-replicate, differentiate into both hepatocyte and cholangiocyte lineages, and repopulate the liver of carbon tetrachloride (CCl_4)-treated immunodeficient mice. *In vitro* gain- and loss-of-function analyses and *in vivo* transplantation analysis were performed. Next, we investigated how TGFBR2 expression is regulated in the hepatoblast fate decision. Finally, we examined whether our findings could be reproduced in delta-like 1 homolog (Dlk1)-positive hepatoblasts obtained from the liver of E13.5 mice. To the best of our knowledge, this study provides the first evidence of c/EBP-mediated regulation of TGFBR2 expression in the human hepatoblast fate decision.

RESULTS

Hepatoblast-like cells are generated from hESCs

First, we investigated whether the hepatoblast-like cells (HBCs), which were differentiated from hESCs as described in supplementary material Fig. S1A, have similar characteristics to human hepatoblasts. We recently found that hESC-derived HBCs could be purified and maintained on human laminin 111 (LN111)-coated dishes (Takayama et al., 2013). The long-term cultured HBC population (HBCs passaged more than three times were used in this study) were nearly homogeneous and expressed human hepatoblast markers such as alpha-fetoprotein (AFP), albumin (ALB), cytokeratin 19 (CK19, also known as KRT19) and EPCAM (Schmelzer et al., 2007) (supplementary material Fig. S1B). In addition, most of the colonies observed on human LN111-coated plates were ALB and CK19 double positive, although a few colonies were ALB single positive, CK19 single positive, or ALB and CK19 double negative (supplementary material Fig. S1C). To examine the hepatocyte differentiation capacity of the HBCs *in vivo*, these cells were transplanted into CCl_4-treated immunodeficient mice. The hepatocyte functionality of the transplanted cells was assessed by measuring secreted human ALB levels in the recipient mice (supplementary material Fig. S1D). Human ALB serum was detected in the mice that were transplanted with the HBCs, but not in the control mice. These results demonstrated that the HBCs generated from hESCs have similar characteristics to human hepatoblasts and would therefore provide a valuable tool to investigate the mechanisms of human liver development. In the present study, HBCs generated from hESCs were used to elucidate the mechanisms of the hepatoblast fate decision.

TGFBR2 expression is decreased in hepatocyte differentiation but increased in cholangiocyte differentiation

The HBCs used in this study have the ability to differentiate into both hepatocyte-like cells [cytochrome P450 3A4 (CYP3A4) positive; Fig. 1B] and cholangiocyte-like cells (CK19 positive; Fig. 1C) (the protocols are described in Fig. 1A). Because the expression pattern of TGFBR2 during differentiation from hepatoblasts is not well known, we examined it in hepatocyte and cholangiocyte differentiation from HBCs. *TGFBR2* was downregulated during hepatocyte differentiation from HBCs (Fig. 1D), but upregulated in cholangiocyte differentiation from HBCs (Fig. 1E). After the HBCs were cultured on Matrigel, the cells were fractionated into three populations according to the level of TGFBR2 expression (TGFBR2-negative, -lo or -hi; Fig. 1F). The HBC-derived TGFBR2-lo cells strongly expressed *αAT* and *CYP3A4* (hepatocyte markers), whereas the HBC-derived TGFBR2-hi cells strongly expressed *SOX9* and integrin β4 (*ITGB4*) (cholangiocyte markers). These data suggest that the TGFBR2 expression level is decreased in hepatic differentiation, but increased in biliary differentiation of the HBCs.

The cell fate decision of HBCs is regulated by TGFβ signals

To examine the function of TGFβ1, β2 and β3 (all of which are ligands of TGFBR2) in the hepatoblast fate decision, HBCs were cultured in medium containing TGFβ1, β2 or β3 (Fig. 2A,B). The expression levels of cholangiocyte marker genes were upregulated by addition of TGFβ1 or TGFβ2, but not TGFβ3 (Fig. 2A), whereas those of hepatocyte markers were downregulated by addition of TGFβ1 or TGFβ2 (Fig. 2B). To ascertain that TGFBR2 is also important in the hepatoblast fate decision, HBCs were cultured in medium containing SB-431542, which inhibits TGFβ signaling (Fig. 2C,D). Hepatocyte marker genes were upregulated by inhibition of TGFβ signaling (Fig. 2C), whereas cholangiocyte markers were downregulated (Fig. 2D). To confirm the function of TGFβ1, β2 and β3 in the hepatoblast fate decision, colony assays of the HBCs were performed in the presence or absence of TGFβ1, β2 or β3 (Fig. 2E). The number of CK19 single-positive colonies was significantly increased in TGFβ1- or β2-treated HBCs. By contrast, the number of ALB and CK19 double-positive colonies was reduced in TGFβ1-, β2- or β3-treated HBCs. These data indicated that TGFβ1 and β2 positively regulate the biliary differentiation of HBCs. Taken together, the findings suggested that TGFBR2 might be a key molecule in the regulation of hepato-bilary lineage segregation.

TGFBR2 plays an important role in the cell fate decision of HBCs

To examine whether TGFBR2 plays an important role in the hepatoblast fate decision, *in vitro* gain- and loss-of-function analysis of TGFBR2 was performed in the HBCs. We used siRNA in knockdown experiments (supplementary material Fig. S2) during HBC differentiation on Matrigel. Whereas TGFBR2-suppressing siRNA (si-TGFBR2) transfection upregulated the expression of hepatocyte markers, it downregulated cholangiocyte markers (Fig. 3A). si-TGFBR2 transfection increased the percentage of asialoglycoprotein receptor 1 (ASGR1)-positive hepatocyte-like cells (Fig. 3B). By contrast, it decreased the percentage of aquaporin 1 (AQP1)-positive cholangiocyte-like cells. These results suggest that TGFBR2 knockdown promotes hepatocyte differentiation, whereas it inhibits cholangiocyte differentiation. Next, we used Ad vector to perform efficient transduction into the HBCs (supplementary material Fig. S3) and ascertained *TGFBR2* gene expression in TGFBR2-expressing Ad vector (Ad-TGFBR2)-transduced cells (supplementary material Fig. S4). Ad-TGFBR2 transduction downregulated the expression of hepatocyte markers, whereas it upregulated cholangiocyte markers (Fig. 3C). Ad-TGFBR2 transduction decreased the percentage of ASGR1-positive hepatocyte-like cells but increased the percentage of AQP1-positive cholangiocyte-like cells (Fig. 3D). These results suggest that TGFBR2 overexpression inhibits hepatocyte differentiation, whereas it promotes cholangiocyte differentiation. Taken together, these results suggest that TGFBR2 plays an important role in deciding the differentiation lineage of HBCs.

To investigate whether hepatoblasts would undergo differentiation in a TGFBR2-associated manner *in vivo*, HBCs transfected/transduced with si-control, si-TGFBR2, Ad-LacZ or Ad-

Development (2014) doi:10.1242/dev.103168

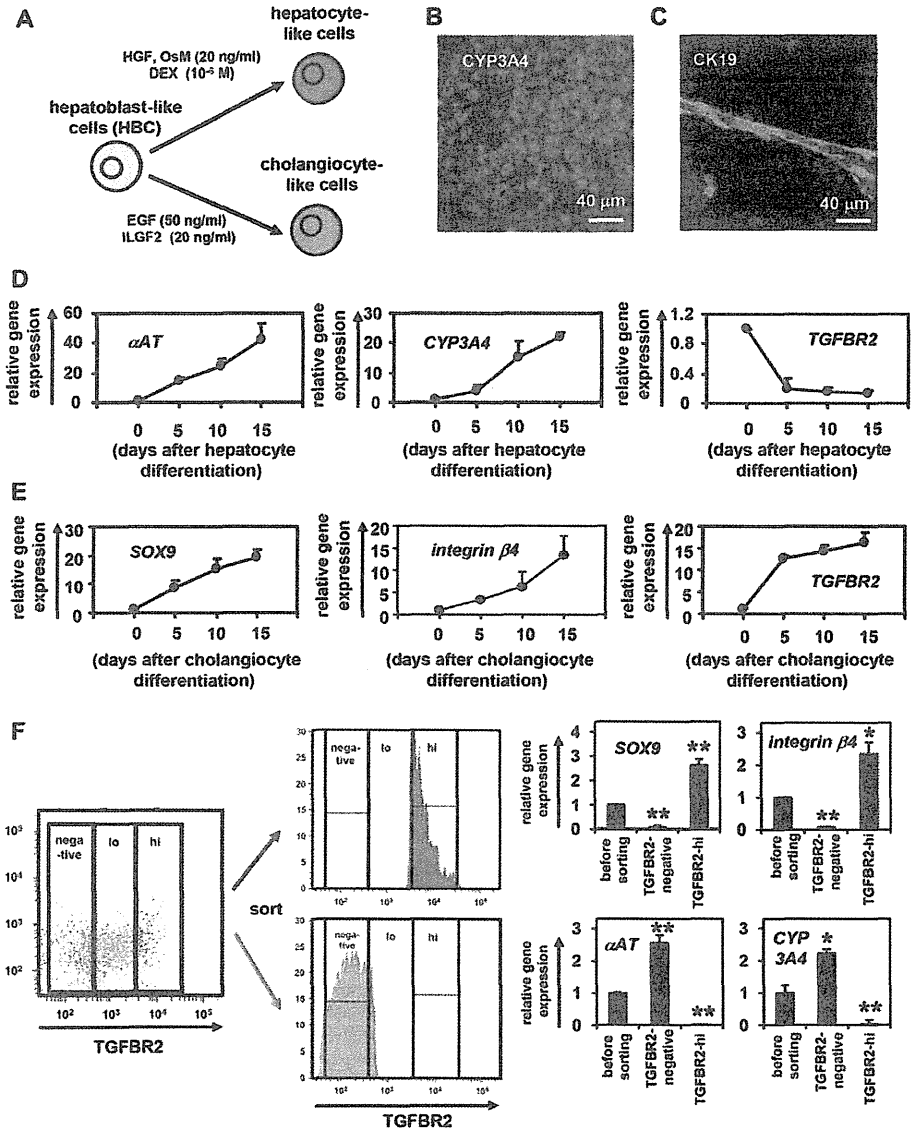

Fig. 1. HBCs can differentiate into both hepatocyte and cholangiocyte lineages. (A) The strategy for hepatocyte and cholangiocyte differentiation from HBCs. (B,C) The HBC-derived hepatocyte-like cells or cholangiocyte-like cells were subjected to immunostaining with anti-CYP3A4 (red, B) or anti-CK19 (green, C) antibodies, respectively. (D,E) Temporal gene expression levels of hepatocyte markers (*αAT* and *CYP3A4*) (D) or cholangiocyte markers (*SOX9* and integrin β4) (E) during hepatocyte or cholangiocyte differentiation as measured by real-time RT-PCR. The temporal gene expression of *TGFBR2* was also examined. The gene expression levels in HBCs were taken as 1.0. (F) HBCs were cultured on Matrigel for 5 days, and then the expression level of TGFBR2 was examined by FACS analysis. TGFBR2-negative, -lo and -hi populations were collected and real-time RT-PCR analysis was performed to measure the expression levels of hepatocyte markers (*αAT* and *CYP3A4*) and cholangiocyte markers (*SOX9* and integrin β4). $^{*}P<0.05$, $^{**}P<0.01$ (compared with 'before sorting'). Error bars indicate s.d. Statistical analysis was performed using the unpaired two-tailed Student's *t*-test ($n=3$).

TGFBR2 were transplanted into CCl_4-treated immunodeficient mice (Fig. 3E,F). Although some of the si-control-transfected or Ad-LacZ-transduced HBCs remained as HBCs (HNF4α and CK19 double positive), most of them showed *in vitro* differentiation toward hepatocyte-like cells (HNF4α single positive) (Fig. 3E, top row). By contrast, Ad-TGFBR2-transduced HBCs were predominantly committed to cholangiocyte-like cells (CK19 single positive) and si-TGFBR2-transfected HBCs were predominantly committed to hepatocyte-like cells (HNF4α single positive) (Fig. 3E, bottom row). Ad-TGFBR2 transduction decreased the percentage of HNF4α-positive hepatocyte-like cells, whereas it increased the percentage of CK19-positive cholangiocyte-like cells (supplementary material Fig. S5). The hepatocyte functionality of the *in vivo* differentiated HBCs was assessed by measuring secreted human ALB levels in the recipient mice (Fig. 3F). Mice that were transplanted with Ad-TGFBR2-transduced HBCs showed lower human ALB serum levels than those transplanted with Ad-LacZ-transduced HBCs, and the mice that were transplanted with si-TGFBR2-transfected HBCs showed higher human ALB serum levels than those transplanted with si-control-transfected HBCs. These data suggest that cholangiocyte or hepatocyte differentiation was promoted by TGFBR2 overexpression or knockdown, respectively. Thus, based on these data from *in vitro* and *in vivo* experiments, TGFBR2 plays an important role in deciding the differentiation lineage of HBCs.

TGFBR2 promoter activity and expression are negatively regulated by c/EBPα and positively regulated by c/EBPβ

A previous study has shown that TGFBR2 expression is upregulated in *Hnf6* knockout mice (Clotman et al., 2005), although we confirmed by ChIP assay that HNF6 does not bind to the *TGFBR2* promoter region (data not shown). Because c/EBPα is important in the hepatoblast fate decision (Suzuki et al., 2003), we expected that c/EBPs might directly regulate TGFBR2 expression. The *TGFBR2* promoter region was analyzed to examine whether TGFBR2 expression is regulated by c/EBPs. Some c/EBP binding sites (supplementary material Fig. S6) were predicted by rVista 2.0 (http://rvista.dcode.org/) (Fig. 4A). By performing a ChIP assay, one

Development (2014) doi:10.1242/dev.103168

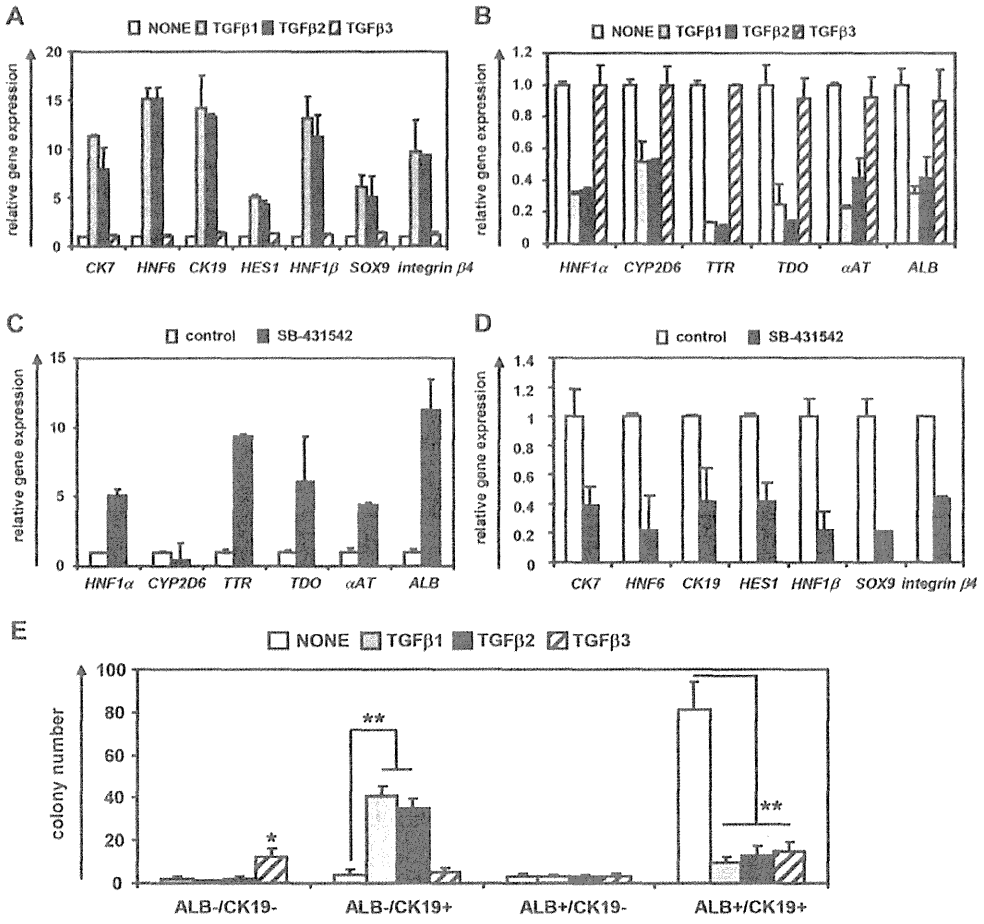

Fig. 2. Hepatocyte and cholangiocyte differentiation from HBCs is regulated by TGFβ signaling. (A,B) HBCs were cultured in differentiation hESF-DIF medium containing 10 ng/ml TGFβ1, TGFβ2 or TGFβ3 for 10 days. The expression levels of cholangiocyte (A) and hepatocyte (B) marker genes were measured by real-time RT-PCR. On the *y*-axis, the gene expression level of cholangiocyte markers in untreated cells (NONE) was taken as 1.0. (C,D) HBCs were cultured in differentiation hESF-DIF medium containing SB-431542 (10 μM) for 10 days. Control cells were treated with solvent only (0.1% DMSO). Expression levels of hepatocyte (C) and cholangiocyte (D) marker genes were measured by real-time RT-PCR. On the *y*-axis, the gene expression level of hepatocyte markers in untreated cells (control) was taken as 1.0. (E) HBC colony formation assay in the presence or absence of 10 ng/ml TGFβ1, TGFβ2 or TGFβ3. HBCs were plated at 200 cells/cm^2 on human LN111-coated dishes. The colonies were separated into four groups based on the expression of ALB and CK19: double-negative, ALB negative and CK19 positive, ALB positive and CK19 negative, and double positive. The numbers represent wells in which the colony was observed in three 96-well plates (total 288 wells). Five days after plating, the cells were fixed with 4% PFA and used for double immunostaining. **P*<0.05, ***P*<0.01 (compared with NONE). Error bars indicate s.d. Statistical analysis was performed using the unpaired two-tailed Student's *t*-test (*n*=3).

c/EBP binding site was found in the *TGFBR2* promoter region (Fig. 4B). A reporter assay of the *TGFBR2* promoter region showed that c/EBPβ activates *TGFBR2* promoter activity, whereas c/EBPα inhibits it (Fig. 4C). In addition, *TGFBR2* expression was downregulated by Ad-c/EBPα transduction, whereas *TGFBR2* was upregulated by Ad-c/EBPβ transduction in HepG2 cells (TGFBR2 positive) (Fig. 4D). We ascertained the expression of *c/EBPα* or *c/EBPβ* (*CEBPA* or *CEBPB* – Human Gene Nomenclature Committee) in the Ad-c/EBPα- or Ad-c/EBPβ-transduced cells, respectively (supplementary material Fig. S4). These results demonstrated that the promoter activity and expression of *TGFBR2* were directly regulated by both c/EBPα and c/EBPβ.

c/EBPs determine the cell fate decision of HBCs via regulation of TGFBR2 expression

To elucidate the relationship between TGFBR2 and c/EBPs (c/EBPα and c/EBPβ) in the hepatoblast fate decision, we first examined the temporal gene expression patterns of *TGFBR2*, *c/EBPα* and *c/EBPβ* in hepatocyte and cholangiocyte differentiation. During hepatocyte differentiation, *TGFBR2* expression was downregulated, whereas *c/EBPα* was upregulated (supplementary material Fig. S7A, top). During cholangiocyte differentiation, *c/EBPα* was downregulated, whereas *TGFBR2* and *c/EBPβ* were upregulated (supplementary material Fig. S7A, bottom). In addition, the ratio of *c/EBPα* to *c/EBPβ* was significantly increased in hepatocyte differentiation, but significantly reduced in cholangiocyte differentiation (supplementary material Fig. S7B). High-level expression of *c/EBPα* was detected in TGFBR2-negative cells, but not in TGFBR2-hi cells (supplementary material Fig. S7C). By contrast, high-level expression of *c/EBPβ* was detected in TGFBR2-hi cells, but not in TGFBR2-negative cells. These results suggest that TGFBR2 is negatively regulated by c/EBPα and positively regulated by c/EBPβ in the differentiation model from HBCs as well as in the HepG2 cell line (Fig. 4).

Development (2014) doi:10.1242/dev.103168

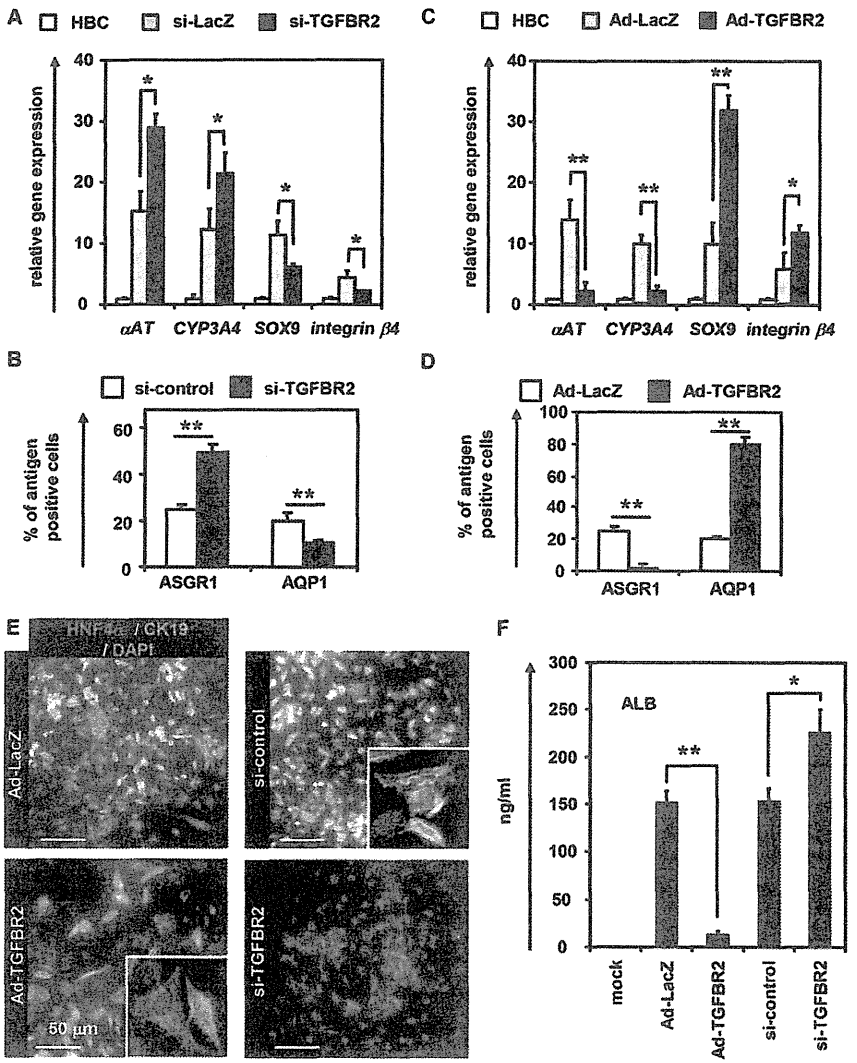

Fig. 3. TGFBR2 regulates bi-directional differentiation of HBCs. (A) HBCs were transfected with 50 nM control siRNA (si-control) or TGFBR2-suppressing siRNA (si-TGFBR2) and cultured in differentiation hESF-DIF medium for 10 days. The expression levels of hepatocyte (*αAT* and *CYP3A4*) or cholangiocyte (*SOX9* and integrin β4) markers were measured by real-time RT-PCR. On the *y*-axis, the gene expression level in HBCs was taken as 1.0. (B) On day 10 after siRNA transfection, the efficiency of hepatocyte or cholangiocyte differentiation was measured by estimating the percentage of ASGR1-positive or AQP1-positive cells, respectively, by FACS analysis. (C) HBCs were transduced with 3000 VPs/cell of Ad-LacZ or Ad-TGFBR2 for 1.5 hours and cultured in differentiation hESF-DIF medium for 10 days. Expression levels of hepatocyte or cholangiocyte marker genes were measured by real-time RT-PCR. On the *y*-axis, gene expression levels in the HBCs was taken as 1.0. (D) On day 10 after Ad vector transduction, the efficiency of hepatocyte or cholangiocyte differentiation was measured by estimating the percentage of ASGR1-positive or AQP1-positive cells, respectively, by FACS analysis. (E,F) The si-control, si-TGFBR2, Ad-LacZ- or Ad-TGFBR2-transfected/transduced HBCs (1.0×10^6 cells) were transplanted into CCl_4-treated (2 mg/kg) *Rag2/Il2rg* double-knockout mice by intrasplenic injection. (E) Expression of human HNF4α (red) and CK19 (green) was examined by double immunohistochemistry 2 weeks after transplantation. Nuclei were counterstained with DAPI (blue). (F) Levels of human ALB in recipient mouse serum were measured 2 weeks after transplantation. **P*<0.05, ***P*<0.01 (compared with Ad-LacZ-transduced or si-control-transfected cells). Error bars indicate s.d. Statistical analysis was performed using the unpaired two-tailed Student's *t*-test (n=3).

ChIP experiments showed that c/EBPα or c/EBPβ is recruited to the *TGFBR2* promoter region containing the c/EBP binding site in hepatocyte-like cells or cholangiocyte-like cells, respectively (Fig. 5A), suggesting that c/EBPα and c/EBPβ oppositely regulate *TGFBR2* promoter activity in the differentiation from HBCs. We confirmed that c/EBPα or c/EBPβ was mainly recruited to the *TGFBR2* promoter region containing the c/EBP binding site in TGFBR-negative or TGFBR2-positive cells, respectively (supplementary material Fig. S7D). Taken together, we concluded that c/EBPα and c/EBPβ are able to regulate the cell fate decision of HBCs via regulation of TGFBR2 expression. During differentiation from HBCs, *TGFBR2* expression was negatively regulated by c/EBPα and positively regulated by c/EBPβ (Fig. 5B). To examine whether c/EBPα or c/EBPβ could regulate the differentiation from HBCs, *in vitro* gain- and loss-of-function analyses were performed. si-c/EBPα transfection downregulated hepatocyte marker gene expression, whereas it upregulated cholangiocyte marker genes (Fig. 5C). By contrast, si-c/EBPβ transfection upregulated hepatocyte marker and downregulated cholangiocyte marker gene expression (Fig. 5C). In accordance, Ad-c/EBPα transduction upregulated hepatocyte marker genes and downregulated cholangiocyte markers (Fig. 5D), whereas Ad-c/EBPβ transduction downregulated hepatocyte markers and upregulated cholangiocyte marker genes. Promotion of hepatocyte differentiation by Ad-c/EBPα transduction was inhibited by Ad-TGFBR2 transduction, whereas inhibition of cholangiocyte differentiation by Ad-c/EBPα transduction was rescued by Ad-TGFBR2 transduction (Fig. 5E). In addition, promotion of hepatocyte differentiation by si-c/EBPβ transfection was inhibited by Ad-TGFBR2 transduction, whereas inhibition of cholangiocyte differentiation by si-c/EBPβ transfection was rescued by Ad-TGFBR2 transduction (Fig. 5F). We further confirmed that inhibition of hepatocyte differentiation by si-c/EBPα-transfection was rescued by si-TGFBR2 transfection (supplementary material Fig. S8). Taken together, these results led us to conclude that c/EBPα and c/EBPβ could determine the cell fate of HBCs by negatively and positively regulating TGFBR2 expression, respectively (supplementary material Fig. S9).

c/EBPs organize the differentiation of fetal mouse hepatoblasts through regulation of TGFBR2 expression

We have demonstrated that c/EBPs may determine the HBC fate decision via regulation of the expression level of TGFBR2. To examine whether our findings could be replicated in native liver

Development (2014) doi:10.1242/dev.103168

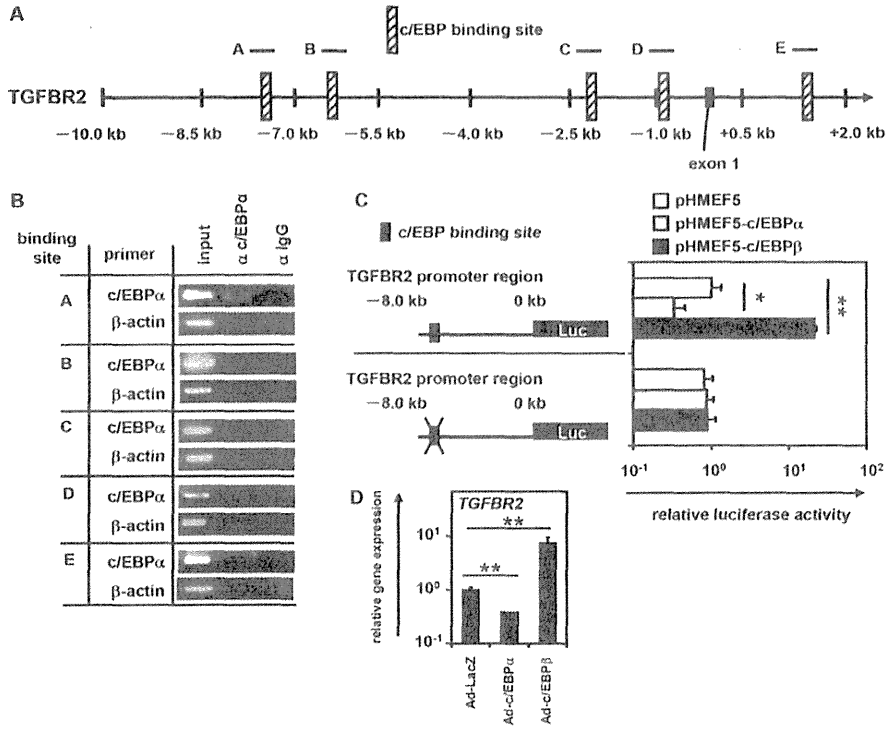

Fig. 4. *TGFBR2* promoter activity and expression are negatively regulated by c/EBPα and positively regulated by c/EBPβ. (A) Candidate c/EBP binding sites (hatched boxes) in the *TGFBR2* promoter region as predicted using rVista 2.0 (see supplementary material Fig. S7). (B) hESCs (H9 cells) were differentiated into hepatoblasts and then a ChIP assay performed. The antibodies and primers employed are summarized in supplementary material Tables S1 and S4. (C) HEK293 cells were transfected with firefly luciferase (Luc) expression plasmids containing the promoter region of *TGFBR2*. In addition, empty plasmid (pHMEF5), c/EBPα expression plasmid (pHMEF5-c/EBPα) or c/EBPβ expression plasmid (pHMEF5-c/EBPβ) was transfected. After 36 hours, a dual luciferase assay was performed. Base pair positions are relative to the translation start site (+1). (D) HepG2 cells (TGFBR2-positive cells) were transduced with 3000 VPs/cell of Ad-LacZ, Ad-c/EBPα or Ad-c/EBPβ for 1.5 hours and cultured for 48 hours. The expression level of *TGFBR2* in HepG2 cells was measured by real-time RT-PCR. On the *y*-axis, the gene expression level in Ad-LacZ-transduced cells was taken as 1.0. $^{*}P<0.05$, $^{**}P<0.01$. Error bars indicate s.d. Statistical analysis was performed using the unpaired two-tailed Student's *t*-test ($n=3$).

development, fetal hepatoblasts were purified from E13.5 mice. The gene expression level of *TGFBR2* in fetal mouse hepatoblasts was negatively or positively regulated by c/EBPα or c/EBPβ, respectively (Fig. 6A,B). The promotion of hepatocyte differentiation by Ad-c/EBPα transduction was inhibited by Ad-TGFBR2 transduction, whereas the inhibition of cholangiocyte differentiation by Ad-c/EBPα transduction was rescued by Ad-TGFBR2 transduction (Fig. 6C). In addition, the promotion of hepatocyte differentiation by si-c/EBPβ transfection was inhibited by Ad-TGFBR2 transduction, whereas the inhibition of cholangiocyte differentiation by si-c/EBPβ transfection was rescued by Ad-TGFBR2 transduction (Fig. 6D). Taken together, these results led us to conclude that c/EBPα and c/EBPβ could determine the cell fate of fetal mouse hepatoblasts by negatively and positively regulating TGFBR2 expression, respectively. Our *in vitro* differentiation system could also prove useful in elucidating the molecular mechanisms of human liver development.

DISCUSSION

The purpose of this study was to better understand the molecular mechanisms of the hepatoblast fate decision in humans. To elucidate the molecular mechanisms of liver development, both conditional knockout mouse models and cell culture systems are useful. For example, DeLaForest et al. demonstrated the role of HNF4α in hepatocyte differentiation using hESC culture systems (DeLaForest et al., 2011). The technology for inducing hepatocyte differentiation from hESCs has recently been dramatically advanced (Takayama et al., 2012a). Because it is possible to generate functional HBCs from hESCs, which can self-replicate and differentiate into both hepatocyte and cholangiocyte lineages (supplementary material Fig. S1 and Fig. 1), the differentiation model of HBCs generated from hESCs should provide a powerful tool for analyzing the molecular mechanisms of human liver development.

In this study, the molecular mechanisms of the hepatoblast fate decision were elucidated using hESC culture systems. HBCs cultured on human LN111 expressed hepatoblast markers (supplementary material Fig. S1) and had the ability to differentiate into both hepatocyte-like cells and cholangiocyte-like cells (Fig. 1). Because a previous study showed that low and high concentrations of TGFβ were required for hepatocyte and cholangiocyte differentiation, respectively (Clotman et al., 2005), we expected that TGFBR2 might contribute to the hepatoblast fate decision. Although TGFβ1, β2 and β3 are all ligands of TGFBR2, TGFβ3 did not promote cholangiocyte differentiation (Fig. 2). This might have been because only TGFβ3 is unable to upregulate the expression of *SOX9*, which is the key factor in bile duct development *in vivo* and cholangiocyte differentiation *in vitro* (Antoniou et al., 2009). We examined the function of TGFBR2 in the hepatoblast fate decision, and found that its overexpression promoted cholangiocyte differentiation, whereas TGFBR2 knockdown promoted hepatocyte differentiation (Fig. 3). Although an exogenous TGFβ ligand was not added to the differentiation medium, the endogenous TGFβ ligand present in Matrigel, which was used in our differentiation protocol, might have bound to TGFBR2. It might also be that the cells committed to the biliary lineage express TGFβ, as a previous study showed that bile duct epithelial cells express TGFβ (Lewindon et al., 2002).

To examine the molecular mechanism regulating TGFBR2 expression, the *TGFBR2* promoter region was analyzed (Fig. 4). *TGFBR2* promoter activity was negatively regulated by c/EBPα and positively regulated by c/EBPβ. c/EBPα overexpression downregulated *TGFBR2* promoter activity in spite of the fact that c/EBPα protein has no repression domain (Yoshida et al., 2006). CTBP1 and CTBP2 (Vernochet et al., 2009) are known to be co-repressors of c/EBPα, and as such constitute candidate co-repressors recruited to the c/EBP binding site in the *TGFBR2* promoter region.

Development (2014) doi:10.1242/dev.103168

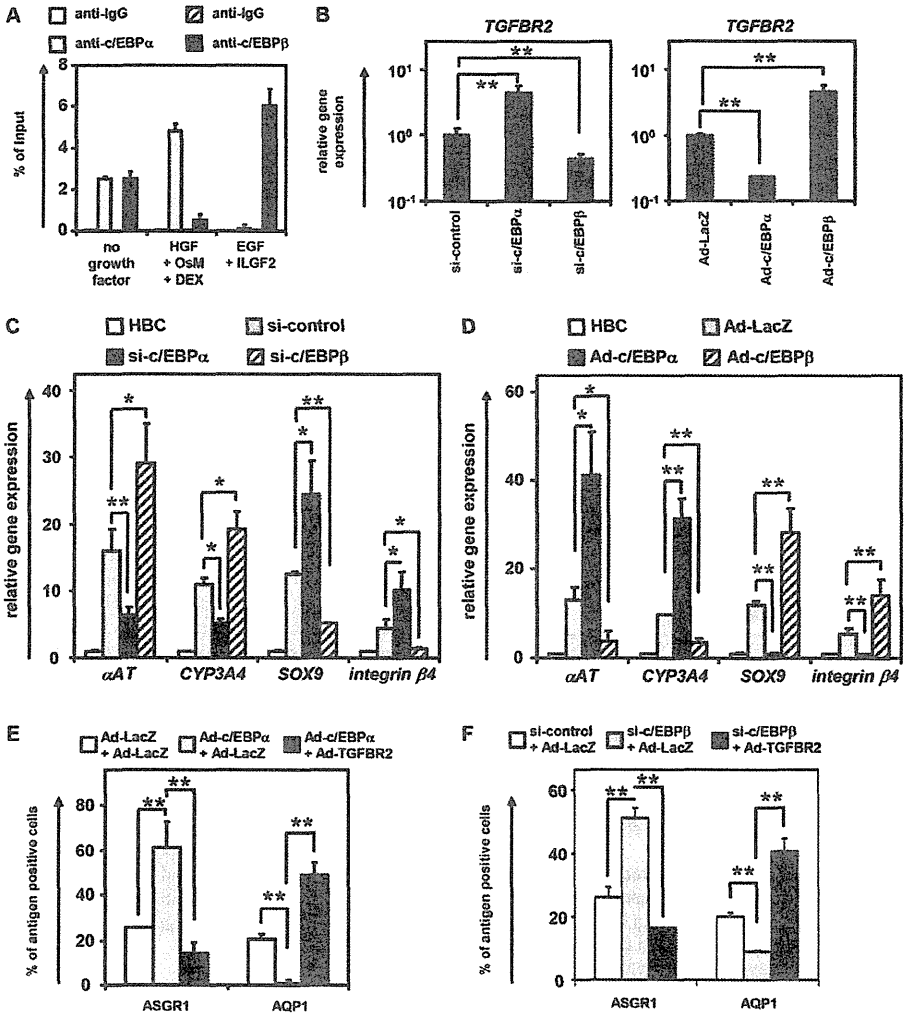

Fig. 5. c/EBPα and c/EBPβ promote hepatocyte and cholangiocyte differentiation by regulating *TGFBR2* expression, respectively. (A) HBCs were differentiated into hepatocyte-like cells or cholangiocyte-like cells according to the scheme outlined in Fig. 1A. On day 10 after hepatocyte or cholangiocyte differentiation, recruitment of c/EBPα or c/EBPβ to the *TGFBR2* promoter region was examined by ChIP assay. (B-D) HBCs were transfected with 50 nM si-control, si-c/EBPα or si-c/EBPβ and cultured in differentiation hESF-DIF medium for 10 days (B left, C). The expression levels of *TGFBR2* and hepatocyte and cholangiocyte markers were then measured by real-time RT-PCR. (B right, D) HBCs were transduced with 3000 VPs/cell of Ad-LacZ, Ad-c/EBPα or Ad-c/EBPβ for 1.5 hours and cultured in differentiation hESF-DIF medium for 10 days. The expression levels of *TGFBR2* and hepatocyte and cholangiocyte markers were then measured by real-time RT-PCR. On the *y*-axis, the gene expression level in the si-control-transfected or Ad-LacZ-transduced cells was taken as 1.0 in B, and levels in HBCs were taken as 1.0 in C and D. (E) HBCs were transduced with 3000 VPs/cell each of Ad-LacZ + Ad-LacZ, Ad-c/EBPα + Ad-LacZ, or Ad-c/EBPα + Ad-TGFBR2 for 1.5 hours and cultured in differentiation hESF-DIF medium for 10 days. The efficiency of hepatocyte or cholangiocyte differentiation was measured by estimating the percentage of ASGR1-positive or AQP1-positive cells, respectively, by FACS analysis. (F) HBCs were transduced with 3000 VPs/cell of Ad-LacZ or Ad-TGFBR2 and then transfected with 50 nM si-control or si-c/EBPβ and cultured in hESF-DIF medium for 10 days. The efficiency of hepatocyte or cholangiocyte differentiation was measured by estimating the percentage of ASGR1-positive or AQP1-positive cells, respectively, by FACS analysis. **P*<0.05, ***P*<0.01. Error bars indicate s.d. Statistical analysis was performed using the unpaired two-tailed Student's *t*-test (*n*=3).

Proteome analysis of c/EBPα would provide an opportunity to identify the co-repressor of c/EBPα. Because large numbers of nearly homogeneous hepatoblasts can be differentiated from hESCs, as compared with the isolation of fetal liver hepatoblasts, hepatocyte differentiation technology from hESCs might prove useful in proteome analysis.

We found that Ad-c/EBPα transduction could promote hepatocyte differentiation by suppressing TGFBR2 expression (Fig. 5). Our findings might thus provide a detailed explanation of the phenotype of *c/EBPα* knockout mice; that is, hepatocyte differentiation is inhibited and cholangiocyte differentiation is promoted in these mice (Yamasaki et al., 2006). We also found that Ad-c/EBPβ transduction could promote cholangiocyte differentiation by enhancing TGFBR2 expression. Because both c/EBPα and c/EBPβ can bind to the same binding site, reciprocal competition for binding is likely to be influenced by regulating c/EBPα or c/EBPβ expression. Therefore, the expression ratio between c/EBPα and c/EBPβ might determine the cell fate of hepatoblasts by regulating the expression level of TGFBR2. We confirmed that our findings could be reproduced in fetal mouse hepatoblasts (Fig. 6). Because a previous study had

Development (2014) doi:10.1242/dev.103168

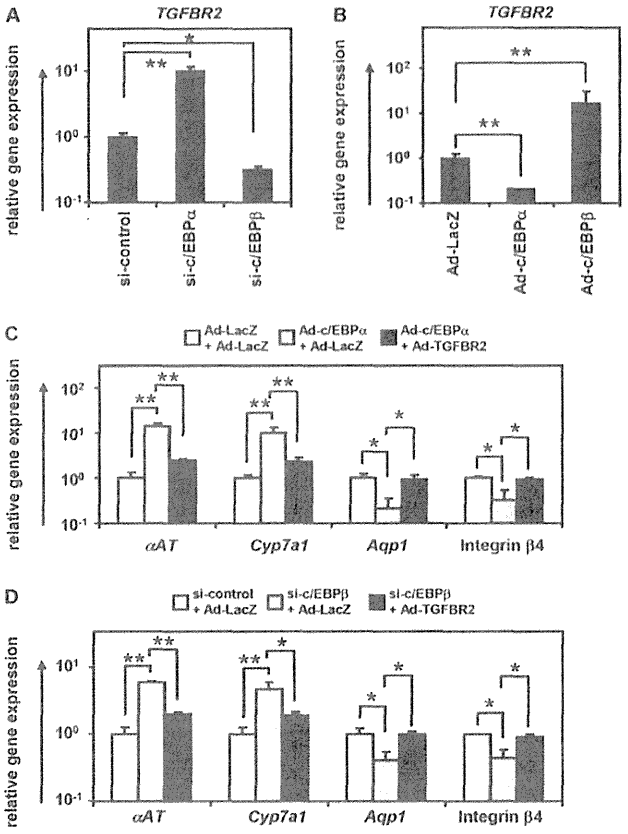

Fig. 6. c/EBPs control the differentiation of fetal mouse hepatoblasts through regulation of TGFBR2 expression. Fetal mouse hepatoblasts (Dlk1-positive cells; the purity was over 98%) were sorted from E13.5 mouse liver. (A) Fetal mouse hepatoblasts were transfected with 50 nM si-control, si-c/EBPα or si-c/EBPβ and cultured for 5 days. The expression of *TGFBR2* was measured by real-time RT-PCR. (B) Fetal mouse hepatoblasts were transduced with 3000 VPs/cell of Ad-LacZ, Ad-c/EBPα or Ad-c/EBPβ for 1.5 hours and cultured for 5 days. The expression of *TGFBR2* was measured by real-time RT-PCR. On the *y*-axis, the gene expression level in the si-control-transfected cells or Ad-LacZ-transduced cells was taken as 1.0. (C) Fetal mouse hepatoblasts were transduced with 3000 VPs/cell each of Ad-LacZ + Ad-LacZ, Ad-c/EBPα + Ad-LacZ, or Ad-c/EBPα + Ad-TGFBR2 for 1.5 hours and cultured for 5 days. On day 5, the expression levels of hepatocyte (*αAT* and *Cyp7a1*) and cholangiocyte (*Aqp1* and integrin β4) markers were measured by real-time RT-PCR. (D) Fetal mouse hepatoblasts were transduced with 3000 VPs/cell of Ad-LacZ or Ad-TGFBR2 and then transfected with 50 nM si-control or si-c/EBPβ and cultured for 5 days. On day 5, the gene levels of hepatocyte (*αAT* and *Cyp7a1*) and cholangiocyte (*Aqp1* and integrin β4) markers were measured by real-time RT-PCR. On the *y*-axis, the gene expression level in the si-control-transfected or Ad-LacZ-transduced cells was taken as 1.0. **P*<0.05, ***P*<0.01. Error bars indicate s.d. Statistical analysis was performed using the unpaired two-tailed Student's *t*-test (*n*=3).

shown that the addition of hepatocyte growth factor (HGF) to hepatoblasts upregulated the expression of c/EBPα and downregulated the expression of c/EBPβ (Suzuki et al., 2003), the ratio between c/EBPα and c/EBPβ might be determined by HGF during hepatocyte differentiation.

In this study, we have identified for the first time that *TGFBR2* is a target of c/EBPs in the hepatoblast fate decision (supplementary material Fig. S9). c/EBPα promotes hepatocyte differentiation by downregulating the expression of TGFBR2, whereas c/EBPβ promotes cholangiocyte differentiation by upregulating TGFBR2 expression. This study might have revealed a molecular mechanism underlying the lineage commitment of human hepatoblasts controlled by a gradient of TGFβ signaling. We believe that similar procedures that adopt the model of human pluripotent stem cell (including human iPS cell) differentiation will be used not only for the elucidation of molecular mechanisms underlying human hepatocyte and biliary differentiation but also for investigating the causes of congenital anomalies of the human liver and biliary tract.

MATERIALS AND METHODS

Ad vectors

Ad vectors were constructed by an improved *in vitro* ligation method (Mizuguchi and Kay, 1998; Mizuguchi and Kay, 1999). The human *c/EBPα* and *c/EBPβ* genes (accession numbers NM_004364 and NM_005194, respectively) were amplified by PCR using the following primers: c/EBPα, Fwd 5′-GCTCTAGATGCCGGGAGAACTCTAACTC-3′ and Rev 5′-GCGGTACCAAACCACTCCCTGGGTCC-3′; c/EBPβ, Fwd 5′-GCATCTAGATTCATGCAACGCCTGGTG-3′ and Rev 5′-ATAGGTACCTAAAATTACCGACGGGCTCC-3′. The human *TGFBR2* gene was purchased from Addgene (plasmid 16622). The human *c/EBPα*, *c/EBPβ* or *TGFBR2* gene was inserted into pBSKII (Invitrogen), resulting in pBSKII-c/EBPα, -c/EBPβ or -TGFBR2. Then, human *c/EBPα*, *c/EBPβ* or *TGFBR2* was inserted into pHMEF5 (Kawabata et al., 2005), which contains the human elongation factor 1α (*EF1α*, also known as *EEF1A1*) promoter, resulting in pHMEF5-c/EBPα, -c/EBPβ or -TGFBR2. pHMEF5-c/EBPα, -c/EBPβ or -TGFBR2 was digested with I-*Ceu*I/PI-*Sce*I and ligated into I-*Ceu*I/PI-*Sce*I-digested pAdHM41-K7 (Koizumi et al., 2003), resulting in pAd-c/EBPα, -c/EBPβ or -TGFBR2. The human *EF1α* promoter-driven *lacZ*- or FOXA2-expressing Ad vectors (Ad-LacZ or Ad-FOXA2, respectively) were constructed previously (Takayama et al., 2012b; Tashiro et al., 2008). All Ad vectors contain a stretch of lysine residues (K7) in the C-terminal region of the fiber knob for more efficient transduction of hESCs, definitive endoderm cells and HBCs, in which transfection efficiency was almost 100%, and the Ad vectors were purified as described previously (Takayama et al., 2012a; Takayama et al., 2011). The vector particle (VP) titer was determined by a spectrophotometric method (Maizel et al., 1968).

hESC culture

The H9 hESC line (WiCell Research Institute) was maintained on a feeder layer of mitomycin C-treated mouse embryonic fibroblasts (Merck Millipore) in ReproStem medium (ReproCELL) supplemented with 5 ng/ml FGF2 (Katayama Kagaku Kogyo). H9 was used following the Guidelines for Derivation and Utilization of Human Embryonic Stem Cells of the Ministry of Education, Culture, Sports, Science and Technology of Japan and the study was approved by the Independent Ethics Committee.

Generation and maintenance of hESC-derived HBCs

Before the initiation of cellular differentiation, the hESC medium was exchanged for a defined serum-free medium, hESF9, and cultured as previously reported (Furue et al., 2008). The differentiation protocol for the induction of definitive endoderm cells and HBCs was based on our previous reports with some modifications (Takayama et al., 2012a; Takayama et al., 2012b; Takayama et al., 2011). Briefly, in mesendoderm differentiation, hESCs were cultured for 2 days on Matrigel Matrix (BD Biosciences) in differentiation hESF-DIF medium, which contains 100 ng/ml activin A (R&D Systems); hESF-DIF medium was purchased from Cell Science & Technology Institute; differentiation hESF-DIF medium was supplemented with 10 μg/ml human recombinant insulin, 5 μg/ml human apotransferrin, 10 μM 2-mercaptoethanol, 10 μM ethanolamine, 10 μM sodium selenite, 0.5 mg/ml bovine fatty acid-free serum albumin (all from Sigma) and 1×B27 Supplement (without vitamin A; Invitrogen). To generate definitive endoderm cells, the mesendoderm cells were transduced with 3000 VPs/cell of FOXA2-expressing Ad vector (Ad-FOXA2) for 1.5 hours on day 2 and cultured until day 6 on Matrigel in differentiation hESF-DIF medium supplemented with 100 ng/ml activin A. For induction of the HBCs, the

definitive endoderm cells were cultured for 3 days on Matrigel in differentiation hESF-DIF medium supplemented with 20 ng/ml BMP4 (R&D Systems) and 20 ng/ml FGF4 (R&D Systems). Transient overexpression of FOXA2 in the mesendoderm cells is not necessary for establishing HBCs, but it is helpful for efficient generation of the HBCs. The HBCs were first purified from the hESC-derived cells (day 9) by selecting attached cells on a human recombinant LN111 (BioLamina)-coated dish 15 minutes after plating (Takayama et al., 2013). The HBCs were cultured on a human LN111-coated dish (2.0×10^4 cells/cm^2) in maintenance DMEM/F12 medium [DMEM/F12 medium (Invitrogen) supplemented with 10% fetal bovine serum (FBS), 1× insulin/transferrin/selenium, 10 mM nicotinamide, 0.1 μM dexamethasone (DEX) (Sigma), 20 mM HEPES, 25 mM $NaHCO_3$, 2 mM L-glutamine, and penicillin/streptomycin] which contained 40 ng/ml HGF (R&D Systems) and 20 ng/ml epidermal growth factors (EGF) (R&D Systems). The medium was refreshed every day. The HBCs were dissociated with Accutase (Millipore) into single cells, and subcultured every 6 or 7 days. The HBCs used in this study were passaged more than three times.

In vitro hepatocyte and cholangiocyte differentiation

To induce hepatocyte differentiation, the HBCs were cultured on a Matrigel-coated dish (7.5×10^4 cells/cm^2) in Hepatocyte Culture Medium (HCM without EGF; Lonza) supplemented with 20 ng/ml HGF, 20 ng/ml Oncostatin M (OsM) (R&D Systems) and 1 μM DEX. To induce cholangiocyte differentiation, the HBCs were cultured in collagen gel. To establish collagen gel plates, 500 μl collagen gel solution [400 μl type I-A collagen (Nitta gelatin), 50 μl 10× DMEM and 50 μl 200 mM HEPES buffer containing 2.2% $NaHCO_3$ and 0.05 M NaOH] was added to each well, and then the plates were incubated at 37°C for 30 minutes. The HBCs (5×10^4 cells) were resuspended in 500 μl differentiation DMEM/F12 medium [DMEM/F12 medium supplemented with 20 mM HEPES, 2 mM L-glutamine, 100 ng/ml EGF and 40 ng/ml ILGF2 (IGF2)], and then mixed with 500 μl of the collagen gel solution and plated onto the basal layer of collagen. After 30 minutes, 2 ml differentiation DMEM/F12 medium was added to the well.

Inhibition of TGFβ signaling

SB-431542 (Santa Cruz Biotechnology), which is a small molecule that acts as a selective inhibitor of activin receptor-like kinase (ALK) receptors [ALK4, ALK5 and ALK7 (also known as ACVR1B, TGFBR1 and ACVR1C)], was used to inhibit TGFβ signaling in HBCs.

Flow cytometry

Single-cell suspensions of hESC-derived cells were fixed with 2% paraformaldehyde (PFA) at 4°C for 20 minutes, and then incubated with primary antibody (supplementary material Table S1) followed by secondary antibody (supplementary material Table S2). Flow cytometry analysis was performed using a FACS LSR Fortessa flow cytometer (BD Biosciences). Cell sorting was performed using a FACS Aria (BD Biosciences).

RNA isolation and reverse transcription (RT)-PCR

Total RNA was isolated from hESCs and their derivatives using ISOGENE (Nippon Gene). cDNA was synthesized using 500 ng total RNA with the SuperScript VILO cDNA Synthesis Kit (Invitrogen). Real-time RT-PCR was performed with SYBR Green PCR Master Mix (Applied Biosystems) using an Applied Biosystems StemOnePlus real-time PCR system. Relative quantification was performed against a standard curve and the values were normalized against the input determined for the housekeeping gene *GAPDH*. Primers are described in supplementary material Table S3.

Immunohistochemistry

Cells were fixed with 4% PFA. After incubation with 0.1% Triton X-100 (Wako), blocking with Blocking One (Nakalai Tesque) or PBS containing 2% FBS, 2% BSA and 0.1% Triton X-100, the cells were incubated with primary antibody (supplementary material Table S1) at 4°C overnight, followed by secondary antibody (supplementary material Table S2) at room temperature for 1 hour. Immunopositive cells were counted in at least eight randomly chosen fields.

HBC colony formation assay

For the colony formation assay, HBCs were cultured at a low density (200 cells/cm^2) on a human LN111-coated dish in maintenance DMEM/F12 medium supplemented with 25 μM LY-27632 (ROCK inhibitor; Millipore).

Transplantation of clonally derived HBCs

Clonally derived HBCs were dissociated using Accutase and then suspended in maintenance DMEM/F12 medium without serum. The HBCs (1×10^6 cells) were transplanted 24 hours after administration of CCl_4 (2 mg/kg) by intrasplenic injection into 8- to 10-week-old *Rag2/Il2rg* double-knockout mice. Recipient mouse livers and blood were harvested 2 weeks after transplantation. Grafts were fixed with 4% PFA and processed for immunohistochemistry. Serum was extracted and subjected to ELISA. All animal experiments were conducted in accordance with institutional guidelines.

ELISA

Levels of human ALB in mouse serum were examined by ELISA using kits from Bethyl Laboratories according to the manufacturer's instructions.

Culture of mouse Dlk1$^+$ cells

Dlk1$^+$ hepatoblasts were isolated from E13.5 mouse livers using anti-mouse Dlk1 monoclonal antibody (MBL International Corporation, D187-4) as described previously (Tanimizu et al., 2003). Dlk1$^+$ cells were resuspended in DMEM/F12 (Sigma) containing 10% FBS, 1× insulin/transferrin/selenium (ITS), 10 mM nicotinamide (Wako), 0.1 μM DEX and 5 mM L-glutamine. Cells were plated on laminin-coated dishes and cultured in medium containing 20 ng/ml HGF, EGF and 25 μM LY-27632 (ROCK inhibitor).

lacZ assay

Hepatoblasts were transduced with Ad-LacZ at 3000 VPs/cell for 1.5 hours. The day after transduction (day 10), 5-bromo-4-chloro-3-indolyl β-D-galactopyranoside (X-Gal) staining was performed as described previously (Kawabata et al., 2005).

Reporter assays

The effects of c/EBPα or c/EBPβ overexpression on *TGFBR2* promoter activity were examined using a reporter assay. An 8 kb fragment of the 5′ flanking region of the *TGFBR2* gene was amplified by PCR using the following primers: Fwd, 5′-CCGAGCTCATGTTTGATGAAGTGTCTAG-CTTCCAAGG-3′; Rev, 5′-GGCTCGAGCCTCGACGTCCAGCCCCT-3′. The fragment was inserted into the *SacI*/*XhoI* sites of pGL3-basic (Promega), resulting in a pGL3-*TGFBR2* promoter region (pGL3-TGFBR2-PR). To generate a *TGFBR2* promoter region containing mutations in the c/EBP binding site, the following primers were used in PCR (mutations are indicated by lowercase letters): Fwd, 5′-CACTAGTATTCAgTG-AtCcgAAAATATGG-3′; Rev, 5′-CACTAGTATTCAgTGAtCcgAAAA-TATGG-3′; this resulted in pGL3-mTGFBR2-PR. HEK293 cells were maintained in DMEM (Wako) supplemented with 10% FBS, penicillin and streptomycin, and 2 mM L-glutamine. In reporter assays, 60 ng pGL3-TGFBR2-PR or pGL3-mTGFBR2-PR was transfected together with 720 ng each expression plasmid (pHMEF5, pHMEF5-c/EBPα and pHMEF5-c/EBPβ) and 60 ng internal control plasmid (pCMV-Renilla luciferase) using Lipofectamine 2000 reagent (Invitrogen). Transfected cells were cultured for 36 hours, and a Dual Luciferase Assay (Promega) was performed according to the manufacturer's instructions.

siRNA-mediated knockdown

Predesigned siRNAs targeting *c/EBPα*, *c/EBPβ* and *TGFBR2* mRNAs were purchased from Thermo Scientific Dharmacon. Cells were transfected with 50 nM siRNA using RNAiMAX (Invitrogen) transfection reagent according to the manufacturer's instructions. As a negative control, we used scrambled siRNA (Qiagen) of a sequence showing no significant similarity to any mammalian gene.

Chromatin immunoprecipitation (ChIP) assay

The ChIP assay kit was purchased from Upstate. Cells were crosslinked using formaldehyde at a final concentration of 1% at 37°C for 10 minutes, and then genomic DNA was fragmented by sonicator. The resulting DNA-protein complexes were immunoprecipitated using the antibodies described in supplementary material Table S1 or control IgG as described in supplementary material Table S2. The precipitated DNA fragments were analyzed by real-time RT-PCR using the primers shown in supplementary material Table S4 to amplify the *TGFBR2* promoter region including the c/EBP binding sites or β-actin locus as a control. The results of quantitative ChIP analysis (Fig. 5A) were expressed as the amount of amplified *TGFBR2* promoter region relative to input DNA taken as 100%.

Statistical analysis

Statistical analysis was performed using an unpaired two-tailed Student's *t*-test. All data are represented as mean ± s.d. (n=3).

Acknowledgements

We thank Natsumi Mimura, Yasuko Hagihara and Hiroko Matsumura for excellent technical support.

Competing interests

The authors declare no competing financial interests.

Author contributions

K. Takayama, K.K. and H.M. developed the concepts or approach; K. Takayama, Y.N., K.O., H.O. and T.Y. performed experiments; K. Takayama, K.K., M.I., K. Tashiro, F.S., T.H., T.O., M.F.K. and H.M. performed data analysis; K. Takayama, K.K. and H.M. prepared or edited the manuscript prior to submission.

Funding

H.M., K.K., M.K.F. and T.H. were supported by grants from the Ministry of Health, Labor, and Welfare of Japan (MEXT). H.M. was also supported by Japan Research Foundation for Clinical Pharmacology, The Uehara Memorial Foundation. K.O. was supported by Special Coordination Funds for Promoting Science and Technology from MEXT. F.S. was supported by Program for Promotion of Fundamental Studies in Health Sciences of the National Institute of Biomedical Innovation (NIBIO). K. Takayama and Y.N. are Research Fellows of the Japan Society for the Promotion of Science.

Supplementary material

Supplementary material available online at
http://dev.biologists.org/lookup/suppl/doi:10.1242/dev.103168/-/DC1

References

Agarwal, S., Holton, K. L. and Lanza, R. (2008). Efficient differentiation of functional hepatocytes from human embryonic stem cells. *Stem Cells* **26**, 1117-1127.

Antoniou, A., Raynaud, P., Cordi, S., Zong, Y., Tronche, F., Stanger, B. Z., Jacquemin, P., Pierreux, C. E., Clotman, F. and Lemaigre, F. P. (2009). Intrahepatic bile ducts develop according to a new mode of tubulogenesis regulated by the transcription factor SOX9. *Gastroenterology* **136**, 2325-2333.

Chen, S. S., Chen, J. F., Johnson, P. F., Muppala, V. and Lee, Y. H. (2000). C/EBPbeta, when expressed from the C/ebpalpha gene locus, can functionally replace C/EBPalpha in liver but not in adipose tissue. *Mol. Cell. Biol.* **20**, 7292-7299.

Clotman, F., Jacquemin, P., Plumb-Rudewiez, N., Pierreux, C. E., Van der Smissen, P., Dietz, H. C., Courtoy, P. J., Rousseau, G. G. and Lemaigre, F. P. (2005). Control of liver cell fate decision by a gradient of TGF beta signaling modulated by Onecut transcription factors. *Genes Dev.* **19**, 1849-1854.

DeLaForest, A., Nagaoka, M., Si-Tayeb, K., Noto, F. K., Konopka, G., Battle, M. A. and Duncan, S. A. (2011). HNF4A is essential for specification of hepatic progenitors from human pluripotent stem cells. *Development* **138**, 4143-4153.

Furue, M. K., Na, J., Jackson, J. P., Okamoto, T., Jones, M., Baker, D., Hata, R., Moore, H. D., Sato, J. D. and Andrews, P. W. (2008). Heparin promotes the growth of human embryonic stem cells in a defined serum-free medium. *Proc. Natl. Acad. Sci. USA* **105**, 13409-13414.

Hansen, A. J., Lee, Y. H., Sterneck, E., Gonzalez, F. J. and Mackenzie, P. I. (1998). C/EBPalpha is a regulator of the UDP glucuronosyltransferase UGT2B1 gene. *Mol. Pharmacol.* **53**, 1027-1033.

Kawabata, K., Sakurai, F., Yamaguchi, T., Hayakawa, T. and Mizuguchi, H. (2005). Efficient gene transfer into mouse embryonic stem cells with adenovirus vectors. *Mol. Ther.* **12**, 547-554.

Kitisin, K., Saha, T., Blake, T., Golestaneh, N., Deng, M., Kim, C., Tang, Y., Shetty, K., Mishra, B. and Mishra, L. (2007). Tgf-Beta signaling in development. *Sci. STKE* **2007**, cm1.

Koizumi, N., Mizuguchi, H., Utoguchi, N., Watanabe, Y. and Hayakawa, T. (2003). Generation of fiber-modified adenovirus vectors containing heterologous peptides in both the HI loop and C terminus of the fiber knob. *J. Gene Med.* **5**, 267-276.

Lewindon, P. J., Pereira, T. N., Hoskins, A. C., Bridle, K. R., Williamson, R. M., Shepherd, R. W. and Ramm, G. A. (2002). The role of hepatic stellate cells and transforming growth factor-beta(1) in cystic fibrosis liver disease. *Am. J. Pathol.* **160**, 1705-1715.

Maizel, J. V., Jr, White, D. O. and Scharff, M. D. (1968). The polypeptides of adenovirus. I. Evidence for multiple protein components in the virion and a comparison of types 2, 7A, and 12. *Virology* **36**, 115-125.

Mizuguchi, H. and Kay, M. A. (1998). Efficient construction of a recombinant adenovirus vector by an improved in vitro ligation method. *Hum. Gene Ther.* **9**, 2577-2583.

Mizuguchi, H. and Kay, M. A. (1999). A simple method for constructing E1- and E1/E4-deleted recombinant adenoviral vectors. *Hum. Gene Ther.* **10**, 2013-2017.

Oe, S., Lemmer, E. R., Conner, E. A., Factor, V. M., Levéen, P., Larsson, J., Karlsson, S. and Thorgeirsson, S. S. (2004). Intact signaling by transforming growth factor beta is not required for termination of liver regeneration in mice. *Hepatology* **40**, 1098-1105.

Plumb-Rudewiez, N., Clotman, F., Strick-Marchand, H., Pierreux, C. E., Weiss, M. C., Rousseau, G. G. and Lemaigre, F. P. (2004). Transcription factor HNF-6/OC-1 inhibits the stimulation of the HNF-3alpha/Foxa1 gene by TGF-beta in mouse liver. *Hepatology* **40**, 1266-1274.

Schmelzer, E., Zhang, L., Bruce, A., Wauthier, E., Ludlow, J., Yao, H. L., Moss, N., Melhem, A., McClelland, R., Turner, W. et al. (2007). Human hepatic stem cells from fetal and postnatal donors. *J. Exp. Med.* **204**, 1973-1987.

Suzuki, A., Iwama, A., Miyashita, H., Nakauchi, H. and Taniguchi, H. (2003). Role for growth factors and extracellular matrix in controlling differentiation of prospectively isolated hepatic stem cells. *Development* **130**, 2513-2524.

Takayama, K., Inamura, M., Kawabata, K., Tashiro, K., Katayama, K., Sakurai, F., Hayakawa, T., Furue, M. K. and Mizuguchi, H. (2011). Efficient and directive generation of two distinct endoderm lineages from human ESCs and iPSCs by differentiation stage-specific SOX17 transduction. *PLoS ONE* **6**, e21780.

Takayama, K., Inamura, M., Kawabata, K., Katayama, K., Higuchi, M., Tashiro, K., Nonaka, A., Sakurai, F., Hayakawa, T., Furue, M. K. et al. (2012a). Efficient generation of functional hepatocytes from human embryonic stem cells and induced pluripotent stem cells by HNF4α transduction. *Mol. Ther.* **20**, 127-137.

Takayama, K., Inamura, M., Kawabata, K., Sugawara, M., Kikuchi, K., Higuchi, M., Nagamoto, Y., Watanabe, H., Tashiro, K., Sakurai, F. et al. (2012b). Generation of metabolically functioning hepatocytes from human pluripotent stem cells by FOXA2 and HNF1α transduction. *J. Hepatol.* **57**, 628-636.

Takayama, K., Nagamoto, Y., Mimura, N., Tashiro, K., Sakurai, F., Tachibana, M., Hayakawa, T., Kawabata, K. and Mizuguchi, H. (2013). Long-term self-renewal of human ES/iPS-derived hepatoblast-like cells on human laminin 111-coated dishes. *Stem Cell Reports* **1**, 322-335.

Tanimizu, N., Nishikawa, M., Saito, H., Tsujimura, T. and Miyajima, A. (2003). Isolation of hepatoblasts based on the expression of Dlk/Pref-1. *J. Cell Sci.* **116**, 1775-1786.

Tashiro, K., Kawabata, K., Sakurai, H., Kurachi, S., Sakurai, F., Yamanishi, K. and Mizuguchi, H. (2008). Efficient adenovirus vector-mediated PPAR gamma gene transfer into mouse embryoid bodies promotes adipocyte differentiation. *J. Gene Med.* **10**, 498-507.

Tomizawa, M., Garfield, S., Factor, V. and Xanthopoulos, K. G. (1998). Hepatocytes deficient in CCAAT/enhancer binding protein alpha (C/EBP alpha) exhibit both hepatocyte and biliary epithelial cell character. *Biochem. Biophys. Res. Commun.* **249**, 1-5.

Vernochet, C., Peres, S. B., Davis, K. E., McDonald, M. E., Qiang, L., Wang, H., Scherer, P. E. and Farmer, S. R. (2009). C/EBPalpha and the corepressors CtBP1 and CtBP2 regulate repression of select visceral white adipose genes during induction of the brown phenotype in white adipocytes by peroxisome proliferator-activated receptor gamma agonists. *Mol. Cell. Biol.* **29**, 4714-4728.

Yamasaki, H., Sada, A., Iwata, T., Niwa, T., Tomizawa, M., Xanthopoulos, K. G., Koike, T. and Shiojiri, N. (2006). Suppression of C/EBPalpha expression in periportal hepatoblasts may stimulate biliary cell differentiation through increased Hnf6 and Hnf1b expression. *Development* **133**, 4233-4243.

Yoshida, Y., Hughes, D. E., Rausa, F. M., III, Kim, I. M., Tan, Y., Darlington, G. J. and Costa, R. H. (2006). C/EBPalpha and HNF6 protein complex formation stimulates HNF6-dependent transcription by CBP coactivator recruitment in HepG2 cells. *Hepatology* **43**, 276-286.

—Foreword—

ウイルスを利用した医療・創薬研究の新展開—ウイルスは貴重なバイオマテリアル—

櫻井文教,*,[a] 近藤昌夫[b]

New Approaches to Drug Discovery Research and Medical Treatment Using Viruses —Viruses Are Valuable Biomaterials—

Fuminori Sakurai*,[a] and Masuo Kondoh[b]

[a]Laboratory of Biochemistry and Molecular Biology; and [b]Laboratory of Bio-Functional Molecular Chemistry, Graduate School of Pharmaceutical Sciences, Osaka University; 1-6 Yamadaoka, Suita, Osaka 565-0871, Japan.

太古の昔より，ウイルスは感染症の原因として人類の脅威であった．例えば，既に紀元前9000年の古代エジプトから天然痘に関する記述が発見されており，実際に天然痘ウイルスに感染した痕跡を残すミイラが発見されている．また，インフルエンザウイルスを原因とするスペイン風邪では，約5000万人の死亡者を出し，ペスト（黒死病）の流行や第二次世界大戦と並び，人類史上最も多くの死亡者を出した大事件であった．現在でも新型インフルエンザなどパンデミックウイルスの出現に備えて世界規模で対策が練られている．

一方でウイルスは，バイオマテリアルとして科学・医療の進歩に多大なる貢献をしてきた．例えば，RNAからDNAを合成する逆転写酵素はRNAウイルスから発見されたし，センダイウイルスによる細胞融合の発見は，その後モノクローナル抗体産生などに応用されている．さらに近年の分子生物学・遺伝子工学の発展は，高機能なウイルスベクターやワクチンの開発を可能にした．現在では，10種類以上の遺伝子組換えウイルスベクターが開発されるとともに，遺伝子組換えワクチンも既に臨床応用されている．ウイルスは，種類によってその特性が大きく異なるため，疾患や研究目的に応じて，利用するウイルスや遺伝子改変法を選択する必要がある．しかし，その基本戦略は“安全性を確保しつつ，用いるウイルスの特徴を最大限生かす”ということで共通している．現在では，ウイルスゲノムの解析を含め各種ウイルスの特性解析が進んだことで，多彩なウイルス改変が可能になるとともに，治療・医薬品開発研究において様々な形でウイルスを利用することが可能となっている．すなわち，医療・創薬研究におけるウイルスの応用性が向上したことで，ウイルスのバイオマテリアルとしての価値が高まっている．

そこで本シンポジウムでは，ウイルスを利用した医療・創薬研究に関して最新の知見を発表して頂いた．以下に本シンポジムのシンポジストと講演タイトルを紹介する．1.「次世代型制限増殖アデノウイルスを利用した血中循環がん細胞検出法の開発」櫻井文教（大阪大学），2.「ウイルス工学を応用した難治がん標的医薬の開発」山村倫子（大阪府立成人病センター），3.「アデノウイルスベクターを利用したC型肝炎研究の新展開」近藤昌夫（大阪大学），4.「「粘膜免疫による交叉防御」と「ワクチン用種ウイルス」に焦点を当てた次世代インフルエンザワクチン研究」岡本成史（医薬基盤研），5.「ウイルスによる自然免疫活性化とその抑制機構」押海裕之（北海道大学）．

最後に本シンポジムの開催並びに誌上シンポジウムの執筆・掲載にあたり，貴重な機会を与えて頂きました日本薬学会第132年会組織委員会・スタッフの先生方並びに日本薬学会役員の先生方，そして今回シンポジストとしてご参加頂きました先生方並びに関係者の皆様に，この場を借りて厚く御礼申しあげます．また，薬学研究者の中でウイルスを扱う研究者は少ないのが現状であるが，本シンポジウムが学生を含む多くの薬学研究者にウイルスに興味を持ってもらう場になることを期待します．

[a]大阪大学大学院薬学研究科分子生物学分野，[b]同生体機能分子化学分野（〒565-0871 大阪府吹田市山田丘1-6）
*e-mail: sakurai@phs.osaka-u.ac.jp
日本薬学会第132年会シンポジウムS41序文